UNIVERSITY OF CALIFORNIA SAN DIEGO

Organic Materials for Haptic Feedback

A dissertation submitted in partial satisfaction of the
requirements for the degree Doctor of Philosophy

in

Nanoengineering

by

Cody Westcott Carpenter

Committee in charge:

Darren Lipomi, Chair
Dimitri Deheyn
Vilayanur S. Ramachandran
Sheng Xu
Liangfang Zhang

2019

The Dissertation of Cody Westcott Carpenter is approved, and it is acceptable in quality and form for publication on microfilm and electronically:

_____

_____

_____

_____

_____

Chair

University of California San Diego

2019

EPIGRAPH

"You're off to great places!
Today is your day!
Your mountain is waiting.
So get on your way!"
-Dr. Seuss

TABLE OF CONTENTS

LIST OF FIGURES

ACKNOWLEDGEMENTS

I would like to acknowledge Professor Darren Lipomi for his support as the chair of my committee. Over the course of the past three years, his guidance has proved to be invaluable.

The Introduction, in part is currently being prepared for submission for publication of the material. Carpenter, C.W., Dhong, C., Lipomi, D.J. The dissertation author was the primary author of this material.

Chapter 1, in full, is a reprint of the material as it appears in Materials Horizons 2018. Carpenter, C.W.[1], Dhong, C.[1], Root, N.[1], Rodriquez, D., Abdo, E., Skelil, K., Alkhadra, M., Ramírez, J., Ramachandran, V.S., Lipomi, D.J. The dissertation author was the primary investigator and author of this paper.

Chapter 2, in full, is a reprint of the material as it appears in Sensors and Actuators A: Physical 2019. Carpenter, C.W.[1], Tan, S.T.M.[1], Keef, C., Skelil, K., Malinao, M., Rodriquez, D., Alkhadra, M.A., Ramírez, J., Lipomi, D.J. The dissertation author was the primary investigator and author of this paper.

Chapter 3, in full, is a reprint of the material as it appears in ACS Omega 2018. Root, S.E., Carpenter, C.W., Kayser, L.V., Rodriquez, D., Davies, D.M., Wang, S., Siew Tan, S.T.M., Meng, Y.S., Lipomi, D.J. The dissertation author was the secondary investigator and author of this material.

Chapter 4, in part is currently being prepared for submission for publication of the material. Carpenter, C.W.[1], Rodriquez[1], D., Tan, S.T.M., Root, N.B., Malinao, M., Skelil,

K., Ramírez, J., Polat, B., Root, S.E., Ramachandran, V.S., Lipomi, D.J. The dissertation author was the primary investigator and author of this material.

VITA

2013	Bachelor of Science, University of California San Diego
2014	Master of Science, University of California San Diego
2014-2016	Scientist, Arytha Biosciencess, LLC.
2019	Doctor of Philosophy, University of California San Diego

PUBLICATIONS

[1] **Carpenter**, **C.W.**[1], Tan, S.T.M.[1], Keef, C., Skelil, K., Malinao, M., Rodriquez, D., Alkhadra, M.A., Ramírez, J., Lipomi, D.J. Healable Thermoplastic for kinesthetic feedback in wearable haptic devices, *Sensors and Actuators A*, 2019, 288, 79-85.

[2] Rodriquez, D., Kohl, J.G., Morel, P., Burrows, K., Favaro, G., Root, S.E., Ramírez, J., Alkhadra, M.A., **Carpenter**, **C.W.**, Fei, Z., Boufflet, P. Martin Heeney, **Lipomi**, D.J. Measurement of Cohesion and Adhesion of Semiconducting Polymers by Scratch Testing: Effect of Side-Chain Length and Degree of Polymerization. *ACS Macro Letters*, 2018, 7, 1003-1009.

[3] **Carpenter, C.W.**[1], Dhong, C.[1], Root, N.[1], Rodriquez, D., Abdo, E., Skelil, K., Alkhadra, M., Ramírez, J., Ramachandran, V.S., Lipomi, D.J., Human ability to discriminate surface chemistry by touch, *Mater. Horiz.*, 2018, 5, 70.

[4] Root, S., **Carpenter, C.W.**, Kayser, L., Rodriquez, D., Tan, M., Davies, D., Meng, S., Lipomi, D.J., Ionotactile stimulation: nonvolatile ionic gels for human–machine interfaces, *ACS Omega*, 2018, 3, 662-666.

[5] Gao, W., **Carpenter**, **C.W.**, Baigude, H., Zhu, W. Universal antivenom based on red blood cell mimicking nanosponges, *Toxicon*, 2016, 117, 104.

[6] Hu, C-M., Fang, R., Wang, K-C., Luk, B., Thamphiwatana, S., Dehaini, D., Nguyen, P., Angsantikul, P., Wen, C., Kroll, A., **Carpenter**, **C.**, Ramesh, M., Qu, V., Patel, S., Zhu, J., Shi, W., Hofman, F., Chen, T., Gao, W., Zhang, K., Chien, S., Zhang, L. "Nanoparticle biointerfacing by platelet membrane cloaking, *Nature,* 2015, 526, 118-121.

[7] Luk, B., Hu, C-M., Fang, R., Dehaini, D., **Carpenter, C.**, Gao, W., Zhang, L., Interfacial interactions between natural RBC membranes and synthetic nanoparticles, *Nanoscale,* 2014, 6, 2730-2737.

[8] Fang, R., Hu, C-M., Chen, K., Luk, B., **Carpenter, C.W.**, Gao, W., Li, S., Zhang, D-E., Lu, W., Zhang, L., Lipid-insertion enables targeting functionalization of erythrocyte membrane-cloaked nanoparticles, *Nanoscale,* 2013, 5, 8884-8888.

[9] Aryal, S., Hu, C-M., Fang, R., Dehaini, D., **Carpenter, C.**, Zhang, D-E., Zhang, L., Erythrocyte membrane-cloaked polymeric nanoparticles for controlled drug loading and release, *Nanomedicine,* 2013, 8, 1271-1280.

[10] Hu, C-M., Fang, R., Luk, B., Chen, K., **Carpenter, C.**, Gao, W., Zhang, K., Zhang, L., 'Marker-of-self' functionalization of nanoscale particles through a top-down cellular membrane coating approach, *Nanoscale,* 2013, 5, 2664-2668.

FIELDS OF STUDY

Major Field: Nanoengineering

Stretchable Electronics
Professor Darren Lipomi

Nanomedicine
Professor Liangfang Zhang

ABSTRACT OF THE DISSERTATION

Organic Materials for Haptic Feedback

by

Cody Westcott Carpenter

Doctor of Philosophy in Nanoengineering

University of California San Diego, 2019

Professor Darren Lipomi, Chair

The skin is the largest organ in the human body. As material scientists, we are hesitant to touch samples out of fear of damaging or contaminating them. This behavior, rational as it is, has prevented us from asking fundamental questions pertaining to our sense of touch that can only be answered using the tools of materials science. This dissertation introduces the methodology of materials science to the toolkit of psychology in order to explore the interface between the human sense of touch and the material world. Here I will

introduce multiple demonstrations that are a part of a larger effort within the Lipomi Research Group to use the tools of organic materials chemistry in haptics research—"organic haptics." The word "haptics" refers to technologies designed to stimulate the tactile and kinesthetic senses. Haptics could enable enhanced forms of physical therapy, realistic virtual environments for education and training, and new art forms that use touch to produce thoughtfulness, imagery, and emotion. Examples include the use of self-assembled monolayers to unveil new limits of tactile perception (i.e. humans can tell the difference between two materials that differ only in their top most layer of molecules), the glass transition temperature of a polymer to interface with the kinesthetic sense, and stretchable conductors for multimodal haptic feedback.

Introduction

Human culture is replete with artifacts that interact with the senses to convey information, or to generate thoughtful or emotional responses. For example, by way of characteristics such as the timbre of a violin, the vibrancy of stained glass, and the effervescence of beer. All of these characteristics are mediated by processes that occur on the molecular scale and nanoscale. The qualities that produce the characteristics regarded as desirable in music, visual art, and food can be understood more or less rigorously with a mix of art and science. A similar level of understanding linking materials science to the tactile sense, however, is underdeveloped. Objects of artwork are not usually designed to be touched. When they are—i.e., in the arts, sculpture and other objects designed to be touched are usually produced to generate a visual object in consciousness. Tactile artwork whose purpose is, instead, to trigger emotions or convey a thoughtful response based on texture are limited by materials that lack dynamism. Among all classes of materials, textiles are perhaps the ones engineered most closely with consideration of the tactile sense. Like most other objects designed to be touched, however, textiles are non-dynamic and thus limited in their level of interaction with human users. With the advent of virtual and augmented reality (VR and AR), technology designed to interface with the tactile sense (the field known as haptics) has drawn group of communities together—e.g., computer scientists, mechanical engineers, and psychologists—that is unusually interdisciplinary. One discipline that is underrepresented, but which has much to say about the development of haptics, is chemistry and materials science.

All tactile sensations arise at an interface between a soft material (i.e., human skin) and the layer of molecules present at the surface of an object. The "feel" of an object is mediated by its bulk mechanical properties, temperature and thermal conductivity, and friction present at the surface, as mediated by intermolecular and surface forces. Materials chemistry is responsible for establishing these parameters, and chemistry at the nanoscale is required to endow them with dynamism. While haptic devices have achieved a remarkable level of sophistication through the creative efforts of computer scientists and mechanical engineers, the actual sensations produced are limited by the modalities in which devices can interact with the peripheral nervous system. These modalities include mechanical vibrations and ultrasound (or some combination), and kinesthetic feedback (i.e., providing physical resistance that mimics a virtual object). Absent from this suite of sensations are those that can only be replicated with molecular dynamism or reconfigurability on the nanoscale: roughness and smoothness, stickiness and sliminess, wetness and dryness, and surfaces that can mimic these sensations with mechanical properties commensurate with the skin. Achieving these characteristics require innovation in chemistry and materials science, particularly in stimulus-responsive (i.e., "active") polymers and nanostructured surfaces.

At the smallest scale, the tactile sense involves the interaction of the skin with the atoms, molecules, and relief structures at the surface of an object. Control over these aspects of a designed object is generally incidental to the intended function or is achieved only by trial and error. One occasionally encounters especially well-made consumer goods for which it is clear that the tactile experience was important to the designer. The use of materials science in improving the tactile experience extends well beyond hand tools and

current consumer electronics, however. The development of materials that change their surface chemistry, mechanical properties, or thermal conductivity with a stimulus, or otherwise provide new ways to couple with the peripheral nervous system (e.g., conductive hydrogels for electrotactile stimulation) would open up many applications in tactical training, medical education, enhanced robotic surgery (and human-enhanced robotics of all types), physical therapy, art, and of course entertainment. For example, tactile blankets for premature infants and sleeping disorders in adults, tactile "theranostics" for sleep apnea and elderly patients prone to falls. Essentially all of the increasing sophistication of haptic technology has occurred without the input of chemists and materials scientists. Design of materials on the molecular scale for tactile interactions—which we have nicknamed "organic haptics"—could enhance these devices by multiplying the range of realistic (or even unknown) sensations that could be generated. We thus believe that the connection between materials science and touch represents a vast, unexplored blue ocean ripe for basic and applied research.

Interdisciplinarity is a word that rightly describes the most attention-worthy research of the 21st century. In no field is this a more apt descriptor than in organic haptics. While the innovative aspects of organic materials science that can elicit a desired tactile response surely require expertise in chemistry, polymer science, and materials engineering, progress cannot be achieved without the ability to work with others in the widest range of disciplines possible. Nanoscientists often include among them researchers whose original training is electrical or mechanical engineering. The role of electrical and mechanical engineering for tactile devices is obvious: one needs to power devices and connect them to external circuitry. Computer science is needed to interface tactile actuators with VR or AR

environments, or robotic tools. The role of mechanical engineering is manifold: one needs to design apparatuses for kinesthetic feedback and also on the basic level to understand contact mechanics. Biology and medicine are needed to understand the ways in which materials and devices interact with the mechanoreceptors in biological tissues. One community with whom researchers in the physical sciences are not used to interacting—and may lack collaborators—is psychology. The tools of psychology, and increasingly neuroscience, are required for (1) experimental design, (2) workup of data to validate significance, and (3) understanding of how tactile interaction with a physical object becomes an object in consciousness. Physical scientists may feel especially uncomfortable with the qualitative nature of subjective experience, and the scatter in data often obtained. Tactile data may, in other words, seem fuzzy to an engineer. In such cases, however, the statistical methods developed in psychology become crucial to tease out actual perception from statistical anomalies. Moreover, physical scientists and engineers not already used to interacting with the medical community must work with experts to design careful studies of human subjects and receive approval from their Institutional Review Boards (IRBs).

Haptics is inherently an interdisciplinary field. While the field is new and the work described in this introduction is nascent, there is a significant amount of work already done on the basic science that provides the groundwork for a future of organic haptics. The scope of this review is on the contact mechanics, psychophysical studies, and complete devices that form the basis for this new field. The topics covered are written to a materials chemist with an interest in the ways molecular and nanoscale forces manifest in human perception. We also hope that the review appeals to psychologists interested in using the tools of materials science to help us bridge the gulf and also to further their own research.

Interdisciplinarity is a vital force in haptic science, and we hope to provide a useful framework for how we can form a new community. This article is largely concerned with haptics of the future.

The Introduction, in part is currently being prepared for submission for publication of the material. Carpenter, C.W., Dhong, C., Lipomi, D.J. The dissertation author was the primary author of this material.

1 Human ability to discriminate surface chemistry by touch

*Materials Horizons 2018

1.1 Abstract

The sense of touch is mediated by the interaction of a soft material (i.e., skin) with the texture and chemistry of an object's surface. Previous work designed to probe the limits of tactile perception has been limited to materials with surface asperities larger than the molecular scale; such materials may also have different bulk properties. We demonstrate in a series of psychophysical experiments that humans can discriminate surfaces that differ by only a single layer of molecules, and can "read" patterns of hydrophobicity in the form of characters in the ASCII alphabet. We design an apparatus that mimics free exploration of surfaces by humans and corroborate the experimental results with a theoretical model of friction that predicts the velocities and pressures that permit discrimination. These results demonstrate that forces produced, while sliding a finger along surfaces, interact with the mechanoreceptors of the skin to allow the brain to discriminate surfaces that differ only by surface chemistry. While we used intentionally simple surface modifications in this study (silanized vs. oxidized silicon), these experiments establish a precedent for using the techniques of materials chemistry in psychology. They also open the door for the use of more sophisticated, molecularly engineered, materials in the future.

1.2 Conceptual Insights

Can humans discriminate between two surfaces that differ by a single layer of

molecules at the surface solely with the sense of touch? This paper seeks to answer this question by combining the tools of surface science, psychophysics, and tribology. As material scientists, we are hesitant to touch samples out of fear of damaging or contaminating them. This behaviour, rational as it is, has prevented us from asking fundamental questions pertaining to our sense of touch that can only be answered using the tools of materials science. To date, psychophysical studies have traditionally been designed using "off-the-shelf" materials that differ in multiple dimensions, which introduce many confounding variables and effects. This paper introduces the methodology of materials science to the toolkit of psychology in order to explore the interface between the human sense of touch and the material world. We found that indeed humans are capable of detecting differences between smooth surfaces that differ only by their topmost layer of molecules (i.e., they have different surface energies). These surfaces are discriminable due to differences in vibrational frequencies generated while sliding. These psychophysical insights are supported using a silicone mock-up of a finger along with a mathematical model.

1.3 Introduction

Tactile perception of an object is influenced by several parameters: its bulk properties (e.g., hardness[1] and thermal conductivity[2]), its surface properties (e.g., roughness[3]), and variables of extrinsic origin (e.g., thin wetting films[4]). When an object is interrogated with a fingertip at a given force and velocity, these properties trigger sensations in the skin[5] as well as the joints of the hand and arm, and as vibrations detected by the ear, to produce tactile images in consciousness. It is known that the skin is capable

of registering minute differences in periodic roughness[3] and thermal properties[2], but the mechanism by which human subjects distinguish objects based only on surface chemistry is not known. Such knowledge is critical in the development of haptic technology using soft, active materials, and would accelerate development of electronic skin[6], instrumented prostheses[7], devices for physical therapy, and enhanced robotic surgery[8]. It may also lay the groundwork for tactile artwork[9] and a neurological understanding of tactile illusions[10].

It is difficult to overstate the importance of the tactile sense in medicine, psychology, and technology. Tactile and variable-friction displays[11], anti-fouling surface coatings[12], and advanced haptic interfaces for virtual and augmented reality[13] require knowledge of how the properties of materials are perceived by touch. Additional factors such as the morphology and hydration of the skin also contribute to the "feel" of an object[4]. Elucidating the mechanisms that influence tactile perception of objects in the environment requires control over the properties of materials on the molecular scale. Recent work to establish a connection between materials science and the tactile sense focused on, for example, the human ability to discriminate surfaces exhibiting nanoscale differences in micron-scale wavy topographies (e.g., akin to judging which sandpaper is finer, but on the nanoscale), while holding surface chemistry constant[3]. Previous studies to determine the contact mechanics of interfaces between human skin and materials exhibiting different surface chemistries (i.e., glass vs. acrylic resin) were confounded by differences in bulk properties (i.e., thermal conductivities and mechanical properties[14]). The effects of surface chemistry alone—with all bulk properties held constant—have not been explored.

Modification of silicon and silicon oxide surfaces using fluorinated alkylsilanes[15] is a ubiquitous approach to control fouling and adhesion in the design of touch screens[12]

and microelectromechanical systems (MEMS)[16]. Silane monolayers do not affect the bulk properties of the substrate, and thus can be used to isolate the effects of surface chemistry. Systematic control over surface chemistry, and the way it modulates surface forces, may establish a molecular basis—and unveil new limits—of tactile perception. The goal of this work was to test whether humans can discriminate objects based on surface chemistry and to establish a framework for discrimination by touch. That is, to develop a theory—supported by psychophysical and mechanical measurements as well as analytical models—to describe how single layers of molecules give rise to adhesion and friction forces that produce differentiable signals in the brain by sliding or tapping a finger across the surface. If it can be shown that humans possess such sensitivity to surface chemistry, it should be possible to encode information spatially that cannot be detected by any sense other than touch. Moreover, such knowledge might stimulate the development of dynamic, reconfigurable materials that can produce a range of sensations for physical therapy, education, and virtual and augmented reality.

1.4 Results and Discussion

We began by determining whether human subjects could discriminate between near atomically smooth silicon wafers (R_a^{Si} = 0.113 nm) with two different surface chemistries. (I) Hydrophobic: passivated with a fluorinated alkyl silane ("FOTS," R_a^{FOTS} = 0.206 nm). (II) Hydrophilic: activated by plasma oxidation ("SiOH," R_a^{SiOH} = 0.203 nm). In each of eight trials, subjects (n = 15) were asked to freely explore a set of three surfaces and identify the one dissimilar surface (the "odd-man-out"[14]) using only their sense of touch (Fig. 1c,

top). Between subjects, FOTS surfaces were wiped thoroughly with isopropanol, while SiOH surfaces were wiped with isopropanol and re-treated with oxygen plasma <1 h before human subject experiments. Washing did not affect the contact angle of the FOTS surfaces, while the SiOH surfaces retained a water contact angle of zero for several hours after plasma treatment. While it may seem "obvious" that humans could detect the differences between these surfaces based on our intuitive sense that "stickiness" increases with surface energy, in reality discriminating these surfaces is not easy, and some subjects could not discriminate between them at all.

We used generalized mixed-effects modeling (GMM; see Methods) to quantify subjects' accuracy of discrimination. Subjects correctly identified the dissimilar surfaces significantly more often than predicted by chance (Fig. 1d, top bar, mean accuracy = 71.7%; Wald Z test, $P < 0.0001$). However, we found a trending inverse correlation between accuracy and moisture of the skin (Fig. 1e; Wald Z test, $P = 0.067$). It should be noted that skin moisture levels increase drastically when contacting impermeable surfaces on the order of 10 s due to the occlusion of eccrine sweat from the glands of glabrous skin, i.e. the hairless skin found on palm and fingers of the hand and the bottoms of the feet[17]. Therefore, moisture measurements taken before engagement with the surface may not always serve as a robust predictor of accuracy during extended free exploration. To eliminate the possible confounding effect of hydration and capillary forces (i.e., to isolate the effect of van der Waals forces), the experiment was repeated with the wafers submerged in deionized water. In this "wet" condition, subjects ($n = 15$, same subjects as the "dry" experiment) could still identify the dissimilar surface significantly more often than predicted by chance (Fig. 1d, middle bar, mean accuracy = 84.17%; Wald Z test, $P <$

0.0001). In fact, subjects were significantly more accurate in the “wet” condition than in the “dry” condition (Wald Z test, $P < 0.05$). However, we cannot eliminate a possible training effect: all subjects in the “wet” experiment had previously experienced the discrimination task in the “dry” experiment, so the increase in accuracy might have resulted from practice. It is clear, nevertheless, that conditions unique to the “dry” experiment were not necessary to perform the discrimination task. This experiment suggests that differences in capillary adhesion between the two surfaces are not necessary to discriminate between surfaces.

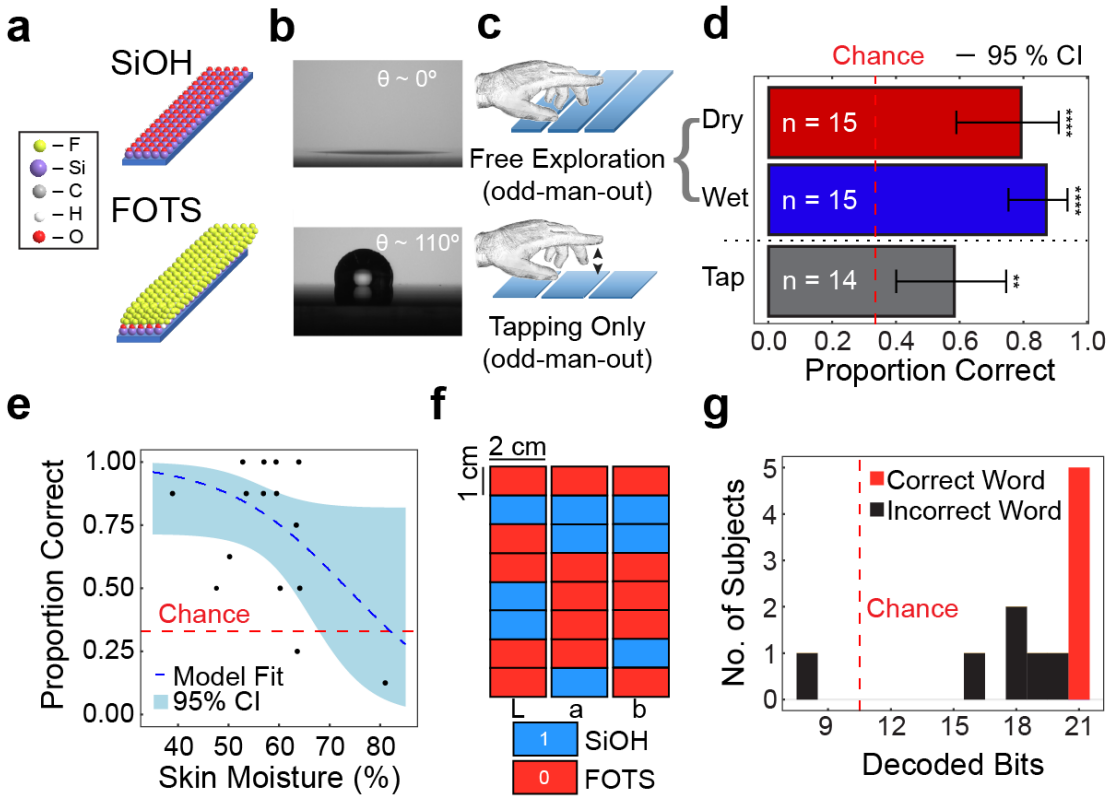

Figure 1. Summary of psychophysical results. a, Schematic diagram of SiOH (top) and FOTS (bottom) surfaces. b, Contact angles of 2 μL water droplets on SiOH (top, static water contact angle = 0°) and FOTS (bottom, static water contact angle = 110°) surfaces. c, Free exploration (top) and tapping only (bottom) in an "odd-man-out" test. d, Behavioural results of discrimination experiments. Data are mean accuracy and 95% confidence interval of the GMM intercept term (see Methods). **P < 0.01, **** P < 0.0001. e, Subject accuracy (*y*-axis) in the "dry" condition as a function of finger pad moisture level (*x*-axis). Red dashed line depicts chance performance. Data are individual subject performance (points), GMM fixed effect (blue dashed line), and 95% confidence interval on fixed effect (see Methods). f, Schematic diagram of "molecular braille" corresponding to rectangular regions of silicon wafers (2 cm × 8 cm) using 1 cm SiOH and FOTS patterned segments to spell the word "Lab" over three separate wafers. g, Plot showing the distribution of successfully decoded bits among subjects (21 successfully decoded bits corresponds to the correct word). Red dashed line depicts chance performance.

Verbal descriptions of the surfaces by the subjects as being "smoother," "stickier," and "slipperier" strongly suggested that friction played a role in the ability of the subject to discriminate between surfaces. It was possible, however, that adhesive forces, felt at the first moment of touching the surface or lifting the finger off the surface, also played a role.

To isolate possible effects of adhesion of the finger to the surface (i.e., tackiness) from those of friction, the experiment was repeated, but subjects were instructed to tap the surfaces rather than explore them freely. Subjects (n = 14, 8 new subjects) could still identify the dissimilar surface significantly more often than predicted by chance (Fig. 1d, bottom bar, mean accuracy = 56.25%; Wald Z test, $P < 0.01$), but significantly less often than in the free exploration conditions (vs. Wet: Wald Z test, $P < 0.0001$; vs. Dry: Wald Z test, $P < 0.01$). It is thus clear that the subjects could perceive molecular differences in surfaces based on adhesion alone, but were significantly more accurate when given the chance to explore surfaces freely (by sliding) rather than restricted to tapping alone. Higher accuracy in free exploration over tapping alone suggests that friction during sliding acted as the primary cue for successful discrimination.

The chemical nature of the interface between the skin and the surface is highly complex and varies bewteen individuals and over time. A finger—even after washing—will deposit eccrine secretions and exfoliated skin. The deposited material consists mostly of inorganic ions, amino acids, and lipids[18]. Free exploration of an initially clean surface means that subjects could pass over a section of the surface that was previously traversed. We thus acknowledge the possibility that secretions could have influenced the ability of human subjects to discriminate the surfaces. We note, however, that these secretions are always present between the skin and the surface whether or not they were on the surface in a previously traversed region. Our measurements and observations suggest that while pre-deposited material may have played a role in the ability of human subjects to discriminate surfaces, the chemistry of the native surface is sufficient. To support this claim, a sinlge subject was asked to perform the odd-man-out test, but was restricted to swiping only

previously unexplored regions of each sample. During this experiment—restricted exploration, as opposed to free exploration—the subject correctly identified the odd-man-out in five of eight trials. Following this experiment, atomic force microscopy and optical microscopy were performed to visualize the deposition on each surface after a single swipe with a length of 2.5 cm (Fig. S3). FOTS surfaces exhibited consistent deposition from the beginning to end of a single swipe, while SiOH surfaces showed less deposition (or simply less smearing of material deposited initially). Contact angles measured on touched regions of each surface maintained a contact angle of zero for SiOH and only a minor increase in the advancing contact angle ($\theta_A = 115°$ initially, $\theta_A = 118°$ after touching) and a decrease in the receding contact angle ($\theta_R = 92°$ initially, $\theta_R = 79°$ after touching) of FOTS surfaces (consistent with increased hydrophilicity after deposition of ions in sweat). Unfortunately, labile material on the surface of the skin is unavoidable and depends on the hydration, surface temperature, and level of keratinization of the skin of each subject. This level of variability makes the degree of human sensitivity to surface chemistry as revealed by the psychophysical experiments even more remarkable.

To test the ability of subjects to distinguish regions of hydrophobicity and hydrophilicity with lateral resolution, we asked subjects to "read" sequences of hydrophilic ("SiOH") and hydrophobic ("FOTS") patches (1-cm long) on a surface representing "1" and "0" bits of the ASCII alphabet, a form of tactile communication akin to braille. Figure 1g shows that 10 of 11 subjects decoded bits of the word "Lab" with accuracy significantly better than chance (binomial tests, all $P < 0.05$) and identified each letter in 4.5 min on average. We note that subjects were aware that the three strings of eight bits combined to form a word rather than a random sequence of letters, which allowed subjects to self-correct

for errors during the experiment. We did not try to test the limit of lateral resolution, but we expect that the accuracy would degrade if the lateral size of the hydrophobic and hydrophilic patches were significantly smaller than 1 cm. We also note that while the FOTS monolayer in principle has a step height of ~1 nm, it is the differences in surface energy (mediated by chemistry), rather than the height, that were being detected by the subjects. (Though remarkably, human subjects can perceive periodic relief features that differ in amplitudes as small as 10 nm.[3])

The next task was to link subjects' abilities to discriminate between surfaces to physical phenomena. Audible sounds produced at various points during free exploration of the surfaces by the subjects were consistent with stick-slip friction. We recorded the sounds (Fig. 2a) and converted them to the frequency domain using a Fourier transform (Fig. 2b). The two surfaces were observed to differ in the sounds produced when interrogated at approximately the same velocity and normal force, as the FOTS surface produced two peaks at 101 and 389 Hz, while the SiOH surface produced one prominent peak at 236 Hz. Vibrational frequencies in this range are detected by the Pacinian corpuscles in the deep dermis, while stretching and movement of the skin (e.g., by sliding the finger along the surface) are registered by the Ruffini endings and Meissner corpuscles[5]. While samples can produce different sounds, most subjects used a light touch that did not produce sounds loud enough to be detected (subjects also wore noise-cancelling headphones that limited auditory cues).

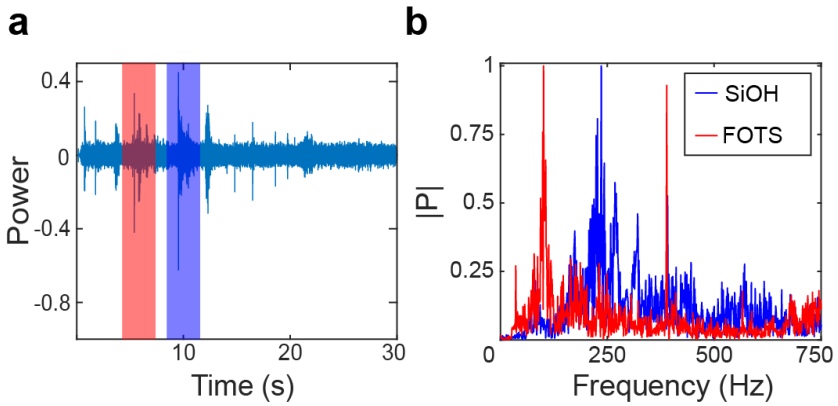

Figure 2. Audible evidence for stick-slip friction. a, Analysis of raw audio signal of finger sliding across FOTS (red box) and SiOH (blue box) surfaces. b, Plot of FFT power analysis of raw audio signals for FOTS (red line) and SiOH (blue line) surfaces.

It is commonly accepted to quantify surfaces based on the static and kinetic coefficients of friction, even though these coefficients are highly dependent on the testing conditions[19], and ignore dynamic instabilities like stick-slip phenomena. The fact that subjects were more accurate in free exploration versus tapping alone would make it tempting to attribute the ability of the subjects to discriminate between the two surfaces to a difference in friction coefficients, considering the static friction coefficients for FOTS and SiOH are quite different (0.13[20] versus 0.44[16]). However, we set out to take a closer look using a mechanical model system since the actual friction forces could be identical under many conditions (i.e., some combinations of normal force and velocity may actually produce similar friction forces).

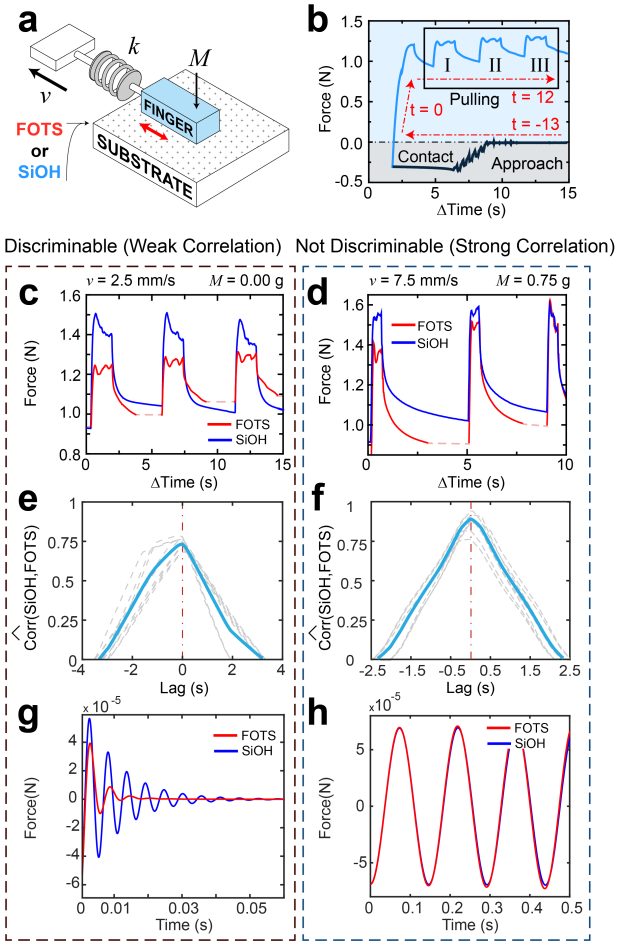

Figure 3. Friction measurements of PDMS on silicon wafers with FOTS or SiOH surfaces. a, Schematic diagram of the apparatus to measure the friction force of a model finger (PDMS block). b, Typical profile of the loading and pulling phases. The first pull after the approach phase was ignored, and then the subsequent three pulls (I-III) were measured. c, d Representative force vs. time traces of the PDMS block on FOTS and SiOH for v = 2.5 mm/s, applied mass = 0 g in (C) and v = 7.5 mm/s, applied mass = 0.75 g. Force traces of samples tested on FOTS have been shifted along the x-axis for easier visual comparison to SiOH. e, f The normalized correlation coefficient of the force vs. time traces in c and d shown in e and f, respectively. The solid line represents the average correlation, and the grey, dashed lines represent the individual correlations. The dashed-red line is a visual guide for symmetry about the x-axis. g, h are the oscillations in force due to sliding friction for a block on surfaces treated with FOTS and SiOH as predicted by the friction model[22].

To investigate the effects of a subject's sliding velocity and applied force on discriminability, we built a custom apparatus drawn schematically in Fig. 3a. This apparatus comprised a force sensor attached to a "finger" made from a block of poly(dimethylsiloxane) (PDMS) with an oxidized surface to reduce its viscoelastic tack.

We mimicked free exploration by testing a range of swiping velocities and normal forces and calculated the cross-correlation between the force traces for the two surfaces. A strong correlation suggests that the surfaces would not be discriminable, while a weak correlation would suggest that the surfaces would be. Since human subjects interrogate objects using free exploration (and unconsciously vary the velocity and force), it is possible that surfaces are only discriminable given certain combinations of velocity and force. Subjects could therefore pass through regions of a hypothetical parameter space of discriminability and non-discriminability multiple times in a single engagement with a surface.

A complete force vs. time trace obtained by the model finger (PDMS block) sliding on a surface is shown in Fig. 3b. The traces of force vs. time had oscillations characteristic of stick-slip behaviour. The first peak is always ignored and the force traces used in the analysis are in the boxed region, labelled I, II and III. Figures 3c and 3d highlight experiments from 2 of the 16 combinations of velocity and force chosen on the basis of whether or not the surfaces were discriminable by cross-correlation. The left-hand column (Fig. 3c, 3e, and 3g) represents a discriminable case, while the right-hand column (Fig. 3d, 3f, and 3h) represents a non-discriminable case. In Fig. 3c (v = 2.5 mm/s and M = 0 g), the force traces of PDMS fingers pulled on FOTS and SiOH-treated surfaces are visually different. M refers to the mass added to the finger, which has a deadweight of 5 g. To avoid possible interference from deposition of unpolymerized material from the PDMS block, we used a new region of the SiOH or FOTS substrate for each measurement. There is a prominent initial spike (stiction) in force[21] on the SiOH surfaces, while the FOTS surface appears to oscillate evenly in force. In Fig. 3d (v = 7.5 mm/s and M = 0.75 g), the traces are visually indistinguishable. We calculated a normalized cross-correlation to quantify the

similarity in force traces. In Fig. 3e, the cross-correlation is asymmetric about *lag* = 0 with a peak correlation value around 0.75 while the cross-correlation in Fig. 3f is more symmetric and the peak correlation is higher at approximately 0.9.

We modelled the friction forces using the simplest model that accounts for stick-slip phenomena[22]. This model introduces the concept of a "state" variable (θ), which accounts for how the friction force varies with the local velocity and displacement of the block, and the time-dependent friction coefficient[23]. Treating the finger as a rigid block connected through a spring to a driver and sliding along one axis, the friction coefficient and the state variable are given in equations (1) and (2):

$$\frac{F_{\parallel}}{F_N} = \mu = \left(\mu_o + \theta + A \ln\left(\frac{v}{v_o}\right)\right) \tag{1}$$

$$\frac{d\theta}{dt} = \left(-\frac{v}{D_c}\right)\left(\theta + B \ln\left(\frac{v}{v_o}\right)\right) \tag{2}$$

where $F_{\parallel}$ and F_N are the parallel force and normal force on the block, t is time, μ is the friction coefficient, v is the velocity of the block, v_o is the motor drive velocity, and A, B, μ_o and D_c are the friction parameters unique to each material (extracted by plotting μ versus v). Oscillations that arise from stick-slip phenomena are shown in Fig. 3g and 3h. In Fig. 3g, we see that the oscillations between the substrates are distinct, while in Fig. 3h, the oscillations overlap both in magnitude and frequency.

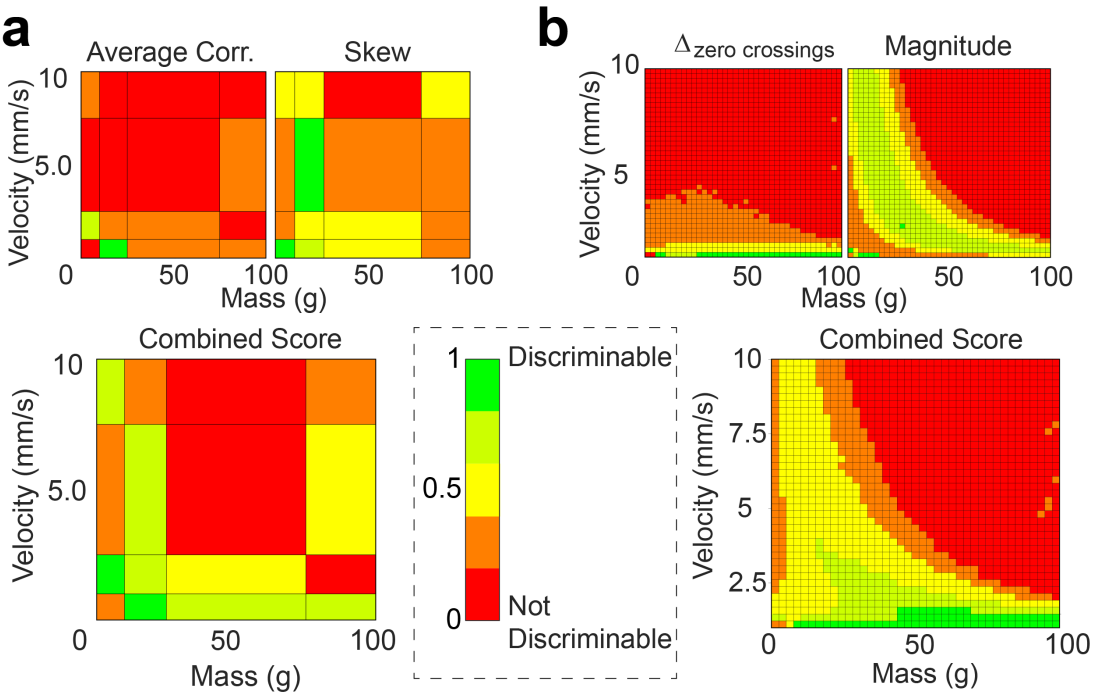

Figure 4. Visualized discriminability score of FOTS and SiOH surfaces from experiments and theory. As shown in the legend with the dashed border, a value of 1 (green) means the FOTS and SiOH surfaces are discriminable, whereas a value of 0 represents surfaces that are not discriminable. a, Experimental results of the cross-correlation when sliding a PDMS block on FOTS and SiOH and two metrics used to evaluate the cross-correlation which were the average value of the cross-correlation, normalized by a maximum cross-correlation value and the skew of the cross-correlation, normalized by the largest skew value in the dataset. The combined score shows the velocities and masses where force traces of FOTS and SiOH are discriminable or not. b, Theoretical oscillations in force due to sliding friction for surfaces on FOTS and SiOH. The two metrics used here are the difference of number of times the direction of slip changes direction (i.e., the number of zero crossings) between FOTS and SiOH, normalized by the maximum possible (0.5), and the percentage of the forces where the FOTS or SiOH is different by a factor of 5. The combined score predicts velocity and applied mass where SiOH and FOTS would be discriminable.

To compare the simple friction model to the experimental output, we created two scoring matrices (Fig. 4). A value of "1" (green) signifies that the substrates exhibit differences in friction forces (and presumably, human perception) while a value of "0" (red) signifies similarity. For the experimental results, we picked a weighted combination of the normalized area under the curve and the normalized skew of the correlation plot, while, for the mathematical model, we picked a weighted combination of the differences

in the number of zero crosses and the differences in magnitude. These weighted combinations give rise to a combined score for the experiments (Fig. 4a) and a predicted one from the model (Fig. 4b), which serve as discrimination matrices. The general trend in both appears to be a sweeping, top-left to bottom-right range in high discriminability, with the largest differences between the substrates at low masses and low velocities. These findings confirm the need to model both experimentally and mathematically the connection between sliding friction and tactile perception, which is not predictable simply from knowledge of the friction coefficient.

1.5 Conclusions

Our results reveal a remarkable human ability to discriminate surfaces based only on surface chemistry: untrained individuals can quickly hone in on the normal forces and sliding velocities required to distinguish surfaces that differ by a single layer of molecules. Subjects can use this ability to decode information—i.e., digital bits and possibly also shapes—that is undetectable by every sense except touch. While adhesion does allow subjects to discriminate between FOTS and SiOH surfaces, the primary mechanism that permits this ability appears to be unequal vibrational frequencies arising from stick-slip friction behaviour triggered by different forces and velocities of interrogation. Interestingly, knowledge of the coefficient of static friction appears to be an insufficient criterion for discriminability. That is, objects with different surface chemistries can "feel" the same with many combinations of forces and velocities, according to the results of both a purpose-built apparatus and an analytical model. Taken together, these results elucidate the limits of the tactile sense and highlight the need for more interdisciplinary research, in

which tactile perception (including its neural and physiological aspects) is investigated using the tools of modern materials science[24]. Better understanding of the relationship between physical properties and human touch perception could spur the development of new, stimulus-responsive materials[25] for haptic feedback and enhanced human-machine interfaces.

Chapter 1, in full, is a reprint of the material as it appears in Materials Horizons 2018. Carpenter, C.W.[1], Dhong, C.[1], Root, N.[1], Rodriquez, D., Abdo, E., Skelil, K., Alkhadra, M., Ramírez, J., Ramachandran, V.S., Lipomi, D.J. The dissertation author was the primary investigator and author of this paper.

1.6 References

[1]. van Kuilenburg, J., Masen, M. A. and van der Heide, E. A review of fingerpad contact mechanics and friction and how this affects tactile perception. *Proc. Inst. Mech. Eng. Part J J. Eng. Tribol.,* 2013, **229,** 243–258.

[2] Ho, H.-N. and Jones, L. A. Contribution of thermal cues to material discrimination and localization. *Percept. Psychophys.,* 2006, **68,** 118–128.

[3] Skedung, L. Arvidsson, M., Chung, J.Y., Stafford, C.M., Berglund, B. and Rutland, M.W. Feeling small: exploring the tactile perception limits. *Sci. Rep.,* 2013, **3,** 2617.

[4] Cornuault, P.-H., Carpentier, L., Bueno, M.-A., Cote, J.-M. and Monteil, G. Influence of physico-chemical, mechanical and morphological fingerpad properties on the frictional distinction of sticky/slippery surfaces. *J. R. Soc. Inter.,* 2015, **12,** 20150495.

[5] Johansson, R. S. and Flanagan, J. R. Coding and use of tactile signals from the fingertips in object manipulation tasks. *Nat. Rev. Neurosci.,* 2009, **10,** 345–59.

[6] Hammock, M. L., Chortos, A., Tee, B. C. K., Tok, J. B. H. and Bao, Z. 25th anniversary article: The evolution of electronic skin (E-Skin): A brief history, design considerations, and recent progress. *Adv. Mater.,* 2013, **25,** 5997–6038.

[7] Raspopovic, S. Capogrosso, M., Petrini, S.M., Bonizzato, M., Rigosa, J., Pino, G.D., Carpaneto, J., Controzzi, M., Boretius, T., Fernandez, E. *et al.* Restoring natural sensory feedback in real-time bidirectional hand prostheses. *Sci. Transl. Med.,* 2014, **6,** 222ra19.

[8] Kuchenbecker, K. J. Gewirtz, J., McMahan, W., Standish, D., Martin, P., Bohren, J., Mendoza, P.J. and Lee, D.I. VerroTouch: High-frequency acceleration feedback for telerobotic surgery. *Lect. Notes Comput. Sci. (including Subser. Lect. Notes Artif. Intell. Lect. Notes Bioinformatics),* 2010, **6191 LNCS,** 189–196.

[9] Gopnik, A. Feel Me. *The New Yorker,* 2016, pp. 56–66.

[10] Lenggenhager, B., Tadi, T., Metzinger, T. and Blanke, O. Video Ergo Sum: Manipulating Bodily. *Science,* 2007, **317,** 1096–1100.

[11] Wiertlewski, M., Fenton, R. and Colgate, J. E. Partial squeeze film levitation modulates fingertip friction. *Proc. Natl. Acad. Sci.,* 2016, **113**.

[12] Sabia, R. and Shashidhar, N. Easy-to-Clean Surfaces for Mobile Devices. Corning Inc., 2010.

[13] Larson, C., Spjut, J., Knepper, R. and Shepherd, R. OrbTouch: Recognizing Human Touch in Deformable Interfaces with Deep Neural Networks. Preprint at https://arxiv.org/abs/1706.02542, 2017.

[14] Gueorguiev, D., Bochereau, S., Mouraux, A., Hayward, V. and Thonnard, J.-L. Touch uses frictional cues to discriminate flat materials. *Sci. Rep.,* 2016, **6,** 25553.

[15] Genzer, J. and Efimenko, K. Creating long-lived superhydrophobic polymer surfaces through mechanically assembled monolayers. *Science,* 2000, **290,** 2130–2133.

[16] Corwin, A. D. Street, M.D., Carpick, R.W., Ashurst, W.R., Starr, M.J., and de Boer, M.P. Friction of Different Monolayer Lubricants in MEMs Interfaces Sandia National Laboratories, 2006.

[17] Pasumarty, S. M., Johnson, S. A., Watson, S. A. and Adams, M. J. Friction of the Human Finger Pad: Influence of Moisture , Occlusion and Velocity. *Tribol. Lett.,* 2011, **44,** 117–137.

[18] Cadd, S., Islam, M., Manson, P. and Bleay, S. Fingerprint Composition and Aging : A Literature Review. *Sci. Justice* 2015, **55,** 219–238.

[19] Ben-David, O. and Fineberg, J. Static friction coefficient is not a material constant. *Phys. Rev. Lett.,* 2011, **106,** 254301.

[20] Khatri, O. P., Devaprakasam, D. and Biswas, S. K. Frictional responses of Octadecyltrichlorosilane (OTS) and 1H, 1H, 2H, 2H-Perfluorooctyltrichlorosilane (FOTS) monolayers self-assembled on aluminium over six orders of contact length scale. *Tribol. Lett.,* 2005, **20,** 235–246.

[21] Lee, D. W., Banquy, X. and Israelachvili, J. N. Stick-slip friction and wear of articular joints. *Proc. Natl. Acad. Sci.,* 2013, **110,** E567-74.

[22] Ruina, A. Slip instability and state variable friction laws. *J. Geophys. Res.,* 1983, **88,** 10359–10370.

[23] Carlson, J. M. and Batista, A. A. Constitutive relation for the friction between lubricated surfaces. *Phys. Rev. E,* 1996, **53,** 4153–4165.

[24] Whitesides, G. M. Physical-Organic Chemistry: A Swiss Army Knife, Isr. J. Chem., 2016, **2138,** 66–82.

[25] Pokroy, B., Kang, S. H., Mahadevan, L. and Aizenberg, J. Self-Organization of a Mesoscale Bristle into Ordered, Hierarchical Helical Assemblies. *Science,* 2009, **323**, 237–241 (2009).

2 Healable Thermoplastic for Kinesthetic Feedback in Wearable Haptic Devices

*Sensors and Actuators A: Physical

2.1 Abstract

The word “haptics” refers to technologies designed to stimulate the tactile and kinesthetic senses. Kinesthesia—the sense of motion—is triggered by imposing forces upon the joints, tendons, and muscles to recreate the geometry and stiffness of objects, as may be useful in physical therapy or virtual reality. Here, we introduce a form of kinesthetic feedback by manipulating the mechanical properties of spandex impregnated with a thermoplastic polymer. Heating or cooling this textile-thermoplastic composite just above or below its glass transition temperature (T_g) dramatically changes its mechanical properties (corresponding to a decrease in storage modulus from 36 MPa to 0.55 MPa). In the form of a glove, the composite can also be healed after inadvertent overextension in its stiffened state by heating it above its T_g. When fitted with thermoelectric devices for active heating and cooling, the flexible or stiffened state of a glove can be perceived by human subjects. As an example of a human-machine interface, the glove is used to control a robotic finger. When the robotic finger makes contact with a wall, a signal is sent to thermoelectric devices in the glove to cool (stiffen the finger) and thus provide kinesthetic feedback to the user.

2.2 Introduction

Kinesthesia refers to the sense associated with moving parts of the body. This sense of self-awareness is enabled by mechanosensory neurons located in muscles, joints, and

tendons.[1] A wearable device that manipulates the kinesthetic sense could have a number of applications in virtual and augmented reality, education, training, and physical therapy. For example, patients experiencing loss of sensation as a result of injury or stroke may require rehabilitation in the form of kinesthetic appliances.[2,3] Here, we introduce a wearable textile-thermoplastic composite in the form of a glove that exhibits changes in stiffness when actively cooled or heated. Changes in the mechanical properties of the material can be perceived by human subjects. This is the first demonstration of manipulation of the glass transition in polymers to produce kinesthetic feedback in a wearable device.

Many technologies known broadly as haptics have been developed to engage both the tactile and kinesthetic senses. Some approaches taken to engage the kinesthetic sense include the use of inertial forces produced by motors to impede a subject's motion.[4] Other devices provide kinesthetic feedback through pneumatic actuation,[5–7] pulley systems,[8] or magneto-rheological fluids.[9] The large pumps and motors required to drive traditional haptic devices can be obtrusive and suggest the need for a new class of sensory and kinesthetic devices which exploits the intrinsic properties of the materials from which the devices are made. One possible strategy to engage the kinesthetic sense that does not in principle require bulky ancillary equipment is the use of variable stiffness materials, which exhibit changes in mechanical properties as a result of a thermal transition. For example, Rich et al. described a conductive thermoplastic elastomer composed of a copolymer of poly(propylene) and poly(ethylene) containing a percolated network of carbon black particles.[10] This material was heated using resistive heating to initiate melting at 73 ºC and a concomitant drop in stiffness as measured by a change in elastic modulus (10 MPa

to 0.7 MPa).[10] Composite foams made of eutectic mixture of tin, indium, and bismuth and a silicone elastomer have also been shown to undergo a large change in elastic modulus (3 MPa to 0.1 MPa) when the metallic component melted at 62 ºC.[11]

Shape-memory materials (e.g., metallic alloys[12] or polymers)[13,14] that switch from a deformed state to a predetermined geometry are another strategy to producing kinesthetic feedback, although these studies did not investigate the ability of human subjects to perceive the change in stiffness. Solazzi et al. show that shape-memory alloys composed of nickel and titanium can be used as actuators to provide tactile feedback through displacement of the skin, but such devices do not generate sensations in the joints and tendons.[12] These materials exhibit large changes in stiffness as well as changes in geometry when thermally activated, while remaining solid.[15] Another thermal transition—advantageous for a wearable device because it too does not involve wholesale melting of the material—is the glass transition of pure or plasticized polymers. This transition, marked by the temperature T_g, corresponds to a transformation of a polymeric material from a rigid, glassy state to a rubbery state in the solid phase[16] (which can be measured by a precipitous drop in storage modulus).

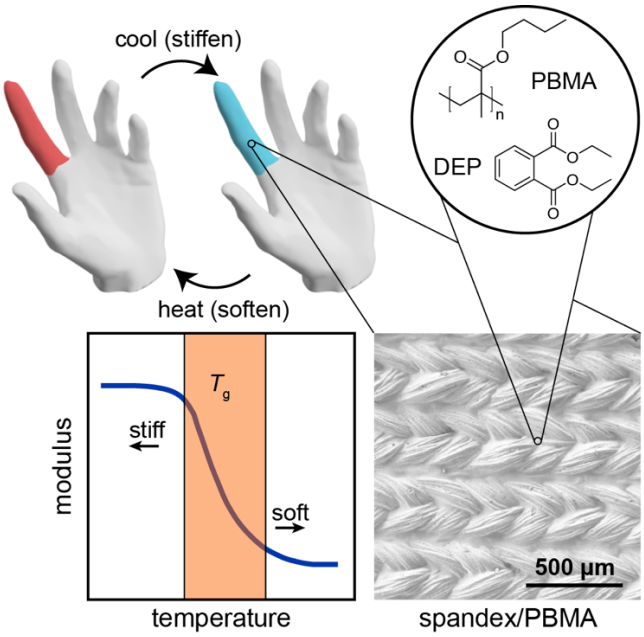

Figure 1. Schematic drawing illustrating the use of variable stiffness material to produce kinesthetic feedback. Active heating and cooling of spandex/PBMA/DEP above and below the T_g causes a change in stiffness of warp-knit spandex infiltrated with PBMA/DEP, shown in the scanning electron microscope (SEM) image. Concept of tuning the T_g of PBMA to be near the temperature of the ambient environment (~23 ºC) or the skin (~32 °C) generates large changes in stiffness with minimal changes in temperature.

Variable stiffness materials have been developed for applications in the field of soft robotics,[17,18] a sub-field of robotics concerned with compliant materials and actuators. When variable stiffness materials are combined with actuators, it is possible to change the shape of a robotic "limb" when heated while being able to support a load once cooled. In the context of a wearable device (Figure 1), the T_g can be tuned to be close to the temperature of the skin: toggling the temperature just above or just below the T_g by a few degrees can trigger a transition between flexible and stiff while the change in temperature is small and, ideally, minimally perceptible. Affecting the rubbery vs. glassy state of a solid polymer can be treated as a passive form of actuation that provides tunable resistance to motion of a body part. A haptic device that interfaces with the kinesthetic sense would ideally exhibit short transition times between soft and stiff states, and not require bulky

external equipment to operate as these devices may impede natural motion of the hand. In this paper, we explore whether it is possible to use the glass transition of a textile-thermoplastic composite material to interface with the kinesthetic sense of human subjects and characterize its thermomechanical properties to provide a foundation from which to design future materials.

2.3 Material Selection

Polymethacrylates have a T_g that can be tuned by varying the length of the side chain (the longer the side chain, the lower the T_g) and can be modified further (decreased) with the use of a plasticizer. We chose poly(butyl methacrylate) (PBMA) as the thermoplastic polymer and diethyl phthalate (DEP) as the plasticizer because this combination can be tuned to exhibit a T_g near the surface temperature of the skin. Solid PBMA is a rigid glassy polymer at room temperature and must be dissolved (e.g., in cyclohexane) or heated to high temperatures for it to be molded. To make this material compatible with wearable applications, 22 wt% PBMA and DEP were incorporated into warp-knit spandex, a polyether–polyurea copolymer. Knitted spandex textiles easily stretch, fit, and conform to the human body and are thus suitable substrates for wearable electronics.[19,20] Textiles made of functional materials are also amenable to scale-up manufacturing where traditional fabrics can be post-processed[21] or fibers made of functionable materials can be incorporated during the weaving and knitting processes.[22]

2.4 Mechanical properties of spandex/PBMA/DEP composites

Given that the spandex/PBMA/DEP composite would be subjected to numerous mechanical stresses when worn as a kinesthetic device on the hand, we next sought to

understand the mechanical properties. We began by performing dynamic mechanical analysis of spandex/PBMA/DEP composites to characterize the T_g as well as the range of stiffnesses that can be achieved in the range of temperatures used to heat and cool the composite. The spandex/PBMA/DEP exhibits a change of nearly two orders of magnitude in storage modulus (36 MPa to 0.55 MPa) over the tested temperature range (9.7 ºC to 47 °C) (Figure 2a). Based on previously reported specific heat capacities of PBMA (using differential scanning calorimetry), we estimated that it would require ~10 mJ g^{-1} to heat the composite from 20 ºC to 35 ºC.[23] We then performed stress–strain measurements on spandex/PBMA/DEP and solid PBMA/DEP. The spandex/PBMA/DEP composite (E = 14 MPa) and PBMA/DEP (E = 18 MPa) exhibited nearly identical mechanical behavior and showed elastic behavior at relatively small strains (ε = 1.5-1.6%) whereas knitted spandex (E = 99 kPa) exhibited purely elastic behavior over the range of tested strains (ε = 0-50% at 10 mm min^{-1}) (Figure 2b). The materials used in this study became stiffer as the strain rate was increased; this behavior is typical of polymers[24] (Figure S1). Spandex/PBMA/DEP composites also showed anisotropic mechanical properties that depended on the orientation of the knit relative to the direction of applied strain (Figure S2). Uniaxial tensile tests (Figure 2b) suggested that the stiffness of spandex/PBMA/DEP composites was due to the PBMA/DEP thermoplastic, which was in its glassy state at the temperature tested.

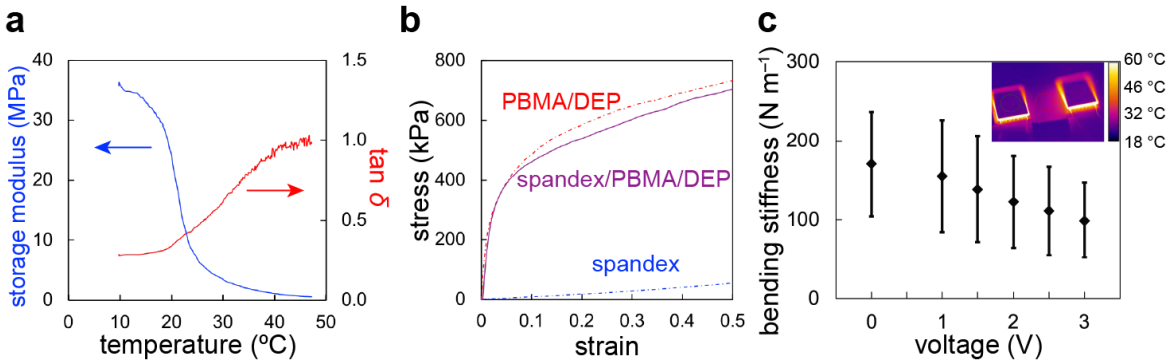

Figure 2. Mechanical properties of spandex/PBMA/DEP composites. (a) Dynamic mechanical analysis of spandex/PBMA/DEP: blue line shows the variation in storage modulus and red line shows the variation in tan δ (i.e., the ratio between loss modulus and storage modulus) as functions of temperature. (b) Tensile stress–strain curves comparing spandex (dotted blue line), pure PBMA/DEP (dotted red line), and the spandex/PBMA/DEP composite (solid purple line) at 10 mm min^{-1}. (c) Plot of bending stiffness in N m^{-1} as a function of applied voltage across thermoelectric devices during active heating above room temperature. (c, Inset) Thermal image of the spandex/PBMA/DEP composite near skin temperature (~32 °C) between two thermoelectric devices used to heat the sample.

Although these tensile tests are useful in quantifying the mechanical properties of the spandex/PBMA/DEP composites, a more relevant metric in applications involving wearable devices is bending stiffness (N m^{-1}) because the material would undergo both tensile and compressive strain during a grasping motion when worn as a glove. Bending stiffness is a measure of the amount of force required to displace a material by a unit of length and it is a function of both the elastic modulus and geometry of the specimen. We performed a three-point bending test (Figure S3 for setup) to measure the stiffness of spandex/PBMA/DEP composites at small deflections (~0.5 mm) and under different heating conditions. As expected, spandex/PBMA/DEP composites showed a steady decrease in bending stiffness as the voltage (and consequently the power, see Figure S4) applied to the thermoelectric devices was increased (heating) (Figure 2c).

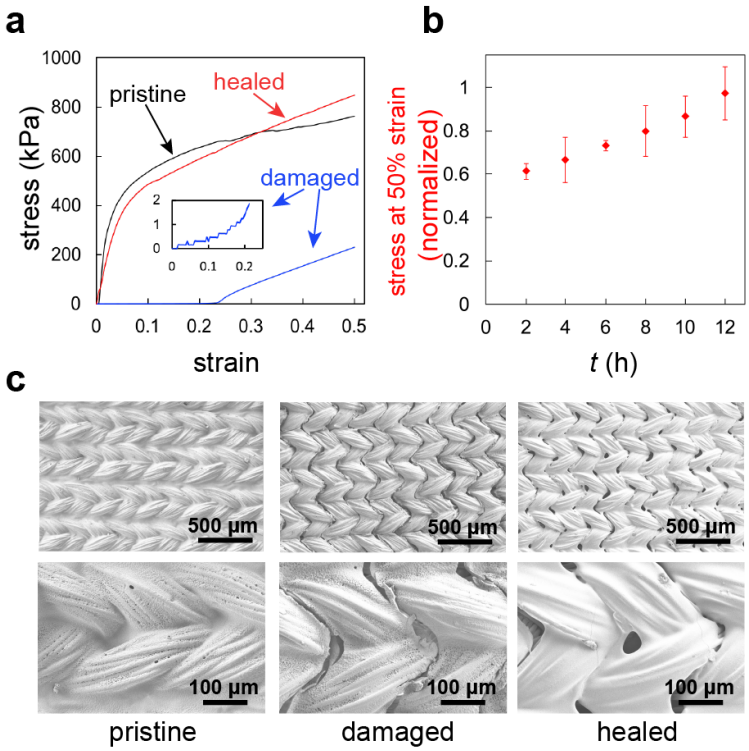

Figure 3. Failure and healing of spandex/PBMA/DEP composites. (a) Stress–strain curves of (black) "pristine," (blue) "damaged," and (red) "healed" spandex/PBMA/DEP samples. (b) Normalized recovery of stress at 50% strain after healing at 90 °C for different amounts of time. (c) SEM images of "pristine," "damaged," and "healed" spandex/PBMA/DEP samples.

2.5 Healing properties of spandex/PBMA/DEP

Spandex/PBMA/DEP composites exhibited elastic behavior at low strain, followed by plastic deformation and fracture of the PBMA/DEP component at higher strains. To measure the change in mechanical properties of spandex/PBMA/DEP composites after overextension (which may occur during normal use as a wearable device), samples were fractured (100% strain) and again subjected to uniaxial tensile strain. One of the advantages of using the thermoplastic PBMA/DEP in providing resistance to motion (the basis of kinesthetic feedback) is that it can be reformed and healed when held at temperatures above T_g for a few hours (Figure 3a). Mechanistically, spandex/PBMA/DEP composites have the ability to recover after being subjected to high tensile strain due to elastic recovery of the

knitted spandex substrate and to heal at low strain due to the ability of PBMA/DEP to flow when heated (i.e., bridge cracks and fill residual void space). Healing of the spandex/PBMA/DEP composite can be repeated many times, since the process merely involves diffusion of polymer chains across fractured interfaces.[25]

To measure the time-dependent healing properties of spandex/PBMA/DEP composites, samples were first stretched by 100% to fracture the PBMA/DEP component. The samples were then placed in an oven at 90 °C (well above T_g) for different amounts of time to promote healing through the reflow of polymer chains across the fractured interface. These samples were strained again to measure mechanical properties (Figure 3a) and to quantify the extent of recovery (Figure 3b). Stress–strain curves of "healed" samples show significant recovery of the spandex/PBMA/DEP composite after 12 h at 90 °C (Figure 3a). The procedure for obtaining stress–strain curves of "damaged" samples differed slightly from the procedure for "healed" samples in that the "damaged" samples were never removed from the grips of the tensile tester. The "damaged" samples were stretched to 100% (to damage them), returned to zero strain, and again stretched to 50% (to give the stress–strain curve shown in blue in Figure 3a). Upon inspection of the stress–strain curves obtained for "damaged" samples, we originally attributed the low stress measured up to ~20% strain to slippage of samples from the grips. A tensile test with a sample marked at each end showed that the sample slipped minimally at the grips and suggested instead that the behavior was due to slack from plastic deformation and fracture of the PBMA/DEP component (Video S1). The stress at 50% strain for "healed" samples was normalized against the stress at 50% strain for "pristine" samples and plotted as a function of healing time (Figure 3b). This parameter (stress at 50% strain) serves as a

measure of the recovery of strength in the material and exhibits a linear dependence on healing time.

To describe qualitatively how spandex/PBMA/DEP composites healed, we performed scanning electron microscopy (SEM) on “pristine,” “damaged,” and “healed” samples. Figure 3c shows PBMA/DEP evenly coats individual spandex fibers and fiber bundles in “pristine” samples, while “damaged” samples show a similar coating with crack formation perpendicular to the applied strain (100% strain). Both “pristine” and “damaged” samples exhibit holes we attribute to evaporation of solvent during preparation. The cracks formed in “damaged” samples of spandex/PBMA/DEP can be attributed to the mechanical failure of PBMA/DEP—as opposed to spandex, which undergoes elastic deformation even at large strain (Figure 2b). Healing through the bridging of cracks as well as the filling of holes was apparent when comparing images of “damaged” and “healed” samples (Figure 3c). We underscore that the composite was able to recover strength by heating only, without the application of external force.

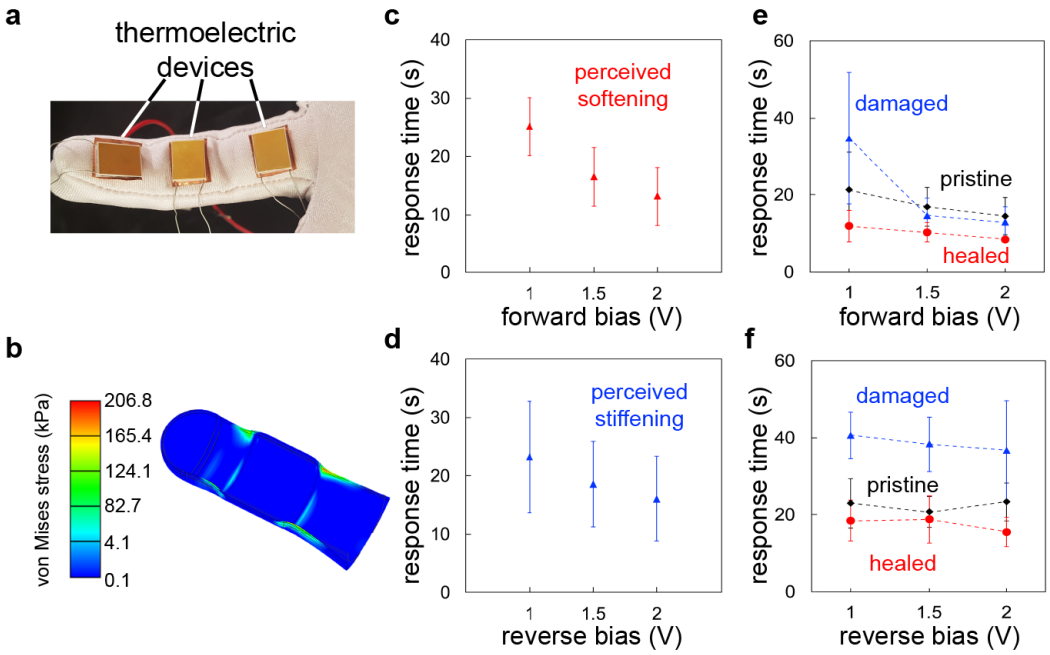

Figure 4. Responses of human subjects to changes in stiffness of the glove. (a) Photograph of the kinesthetic glove fitted with thermoelectric devices. (b) Finite element analysis (FEA) of predicted stress concentration during bending of a finger of the glove. Response times of perceived (c) softening and (d) stiffening as a function of voltage applied to the thermoelectric devices (n = 2 subjects, 30 samples per reported mean and s.d.). Comparison of perceived (e) softening and (f) stiffening times of the kinesthetic glove in "pristine" (black), "damaged" (blue), and "healed" (red) conditions (90 °C for 17 h) (n = 1 subject, 10 samples per reported mean and s.d.).

2.6 Human subject experiments

We fabricated a spandex/PBMA/DEP composite glove fitted with thermoelectric devices to deliver kinesthetic feedback to a human subject (Figure 4a). To fabricate the device, we placed a spandex glove on a mannequin hand (wrapped in Teflon to prevent irreversible adhesion) and painted the bottom of the hand and fingers as well as the sides of each finger with a 0.1 g/mL solution of PBMA in cyclohexane containing 6 wt% DEP. The top side of the spandex glove was left unpainted to allow for elastic recovery (i.e., to bring the glove back to its original shape after bending). The glove was left to dry in ambient conditions for 24 h. Thermoelectric devices were fixed to the bottom side of a

single finger between the joints using double-sided copper tape and sealed along the edges with clear silicone sealant (Loctite). Heating and cooling of the thermoelectric devices was determined by the direction of applied voltage across the thermoelectric devices (forward bias = heating, reverse bias = cooling). The direction of bias was controlled by an Arduino microcontroller, custom breadboard, and an external power source. Softening trials began at room temperature, while stiffening trials began at the end of softening trials when the glove was at an elevated temperature. Finite element analysis (FEA) of this material showed that stress concentrates around the finger joints, which highlights the importance of coating the glove in these regions to maximize kinesthetic feedback (Figure 4b).

To characterize how fast subjects respond to changes in material stiffness, two subjects were asked to continuously bend and unbend the finger inside the glove (fitted with thermoelectric devices) and to report when the glove felt softer or stiffer. Subjects reacted with shorter response times to changes in the stiffness of the material as the forward bias across the thermoelectric devices increased (Figure 4c). Subjects showed a similar decrease in response time as the reverse bias increased when the glove transitioned from a compliant state to a rigid state (Figure 4d). Figures 4c and 4d show that there is wide variation in the response times of human subjects to the change in stiffness of spandex/PBMA/DEP. One possible explanation is that the large distance (~3 mm) between the thermoelectric devices and the joints of the glove, i.e. where stress concentrates at the joints as observed in the FEA results of Figure 4b, combined with the low thermal conductivity of polymers, result in long switching times between soft and stiff states of the textile-thermoplastic composite. A similar experiment was performed to test the effects of plastic deformation of the kinesthetic glove on the ability of a subject to perceive a change

in stiffness. One subject was asked to form a clenched fist to deform the glove past the elastic limit (to damage the PBMA/DEP component) and to repeat each response-time experiment (Figure 4e and 4f). Damage of the glove had a pronounced effect on perceived stiffening times where response times were ~20 s longer than the response times of the "pristine" glove (Figure 4f). Figure 4f also shows that when the experiment was repeated with a "healed" glove (glove placed in an oven at 90 °C for 17 h), the response times returned to the response times of the "pristine" glove.

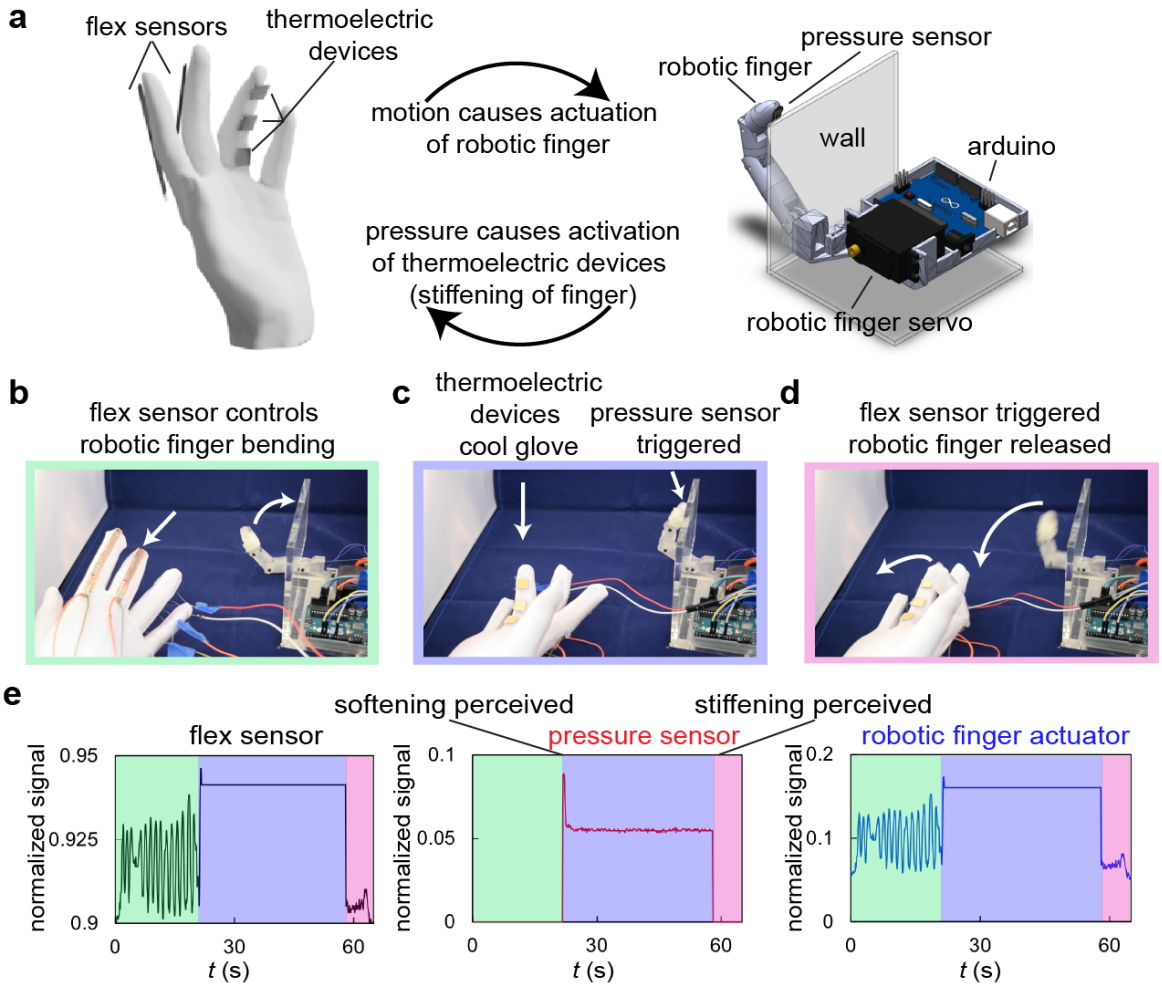

Figure 5. Two-way communication of kinesthetic glove with robotic finger. (a) Schematic diagram. (b-d) Still images (corresponding to Video S2) of each stage of the demonstration; softening (green), stiffening (purple), and re-softening (pink). (e) Normalized sensor data of (left, black line) the flex sensor on the middle finger, (middle, red line) pressure sensor on the robot fingertip, and (right, blue line) the robotic actuator used to retract and extend the robotic finger in response to the flex sensor (middle finger). Signal processing was performed by using an analog-to-digital converter to discretize a range of analog signals (0-5 V) to a range of digital bits (0-1024 bits). Each reading was then normalized by the maximum bit value (1024).

2.7 Robotic finger demonstration

The glove was then equipped with flex sensors to control and receive kinesthetic feedback from a robotic finger. The robotic finger bent in response to flex sensors on the glove and contacted an acrylic wall when bent completely (Figure 5a). When the robotic

finger was in contact with the wall (measured by a pressure sensor on the robotic fingertip) the thermoelectric devices cooled (stiffened) the glove. Otherwise, the thermoelectric devices heated (softened) the glove. Three fingers of the glove were instrumented for different purposes. (1) The role of the middle finger was to control the bending motion of the robotic finger (Figure 5b). (2) The role of the ring finger was to receive kinesthetic feedback induced by heating or cooling of the glove (Figure 5c). (3) The role of the index finger was to signal the robotic finger to break contact with the wall once the subject had perceived that the glove had stiffened (Figure 5d). For this demonstration, we used different fingers to control the motion of the robotic finger (middle finger) and to receive kinesthetic feedback (ring finger) because there was a risk that subjects would inadvertently overbend the finger used to control the robotic finger. Overbending would damage the composite material in its glassy state. In a realistic scenario, however, control of the robotic hand or virtual object would be combined with kinesthetic feedback in the same finger.

We began the first stage (softening) of the demonstration (Figure 5b and 5e, green regions) by applying a forward bias to the thermoelectric devices to heat the kinesthetic glove. The subject was then asked to slightly bend and unbend both the ring and middle fingers cyclically (Figure 5e, oscillatory signal arising from the flex sensor on the middle finger) until the subject perceived that the ring finger of the glove had softened. Once the subject perceived softening of the glove, the subject was asked to bend the middle finger until the robotic finger made contact with the wall. Contact of the robotic finger with the wall was registered by the pressure sensor at the tip of the robotic finger (Figure 5e, signal peak of the pressure sensor). This contact automatically initiated the second stage (stiffening) of the demonstration (Figure 5c and 5e, purple regions), where a reverse bias

was applied across the thermoelectric devices to actively cool (stiffen) the glove. The subject was again asked to bend and unbend the ring finger (Figure 5c and 5e, purple regions) until the subject perceived the glove had stiffened. During this stage, the robotic finger was programmed to ignore the bending motion of the flex sensor on the middle finger (marked by the absence of the oscillatory signal in the purple region of the flex sensor) to give the thermoelectric devices enough time to sufficiently cool the glove. Once the subject perceived the glove had stiffened, the subject was asked to bend the index finger. The signal of the flex sensor on the index finger caused the robotic finger to break contact with the wall (Figure 5b and Figure 5e, highlighted by the signal drop in pressure sensor signal). This break in contact triggered the third stage (re-softening) of the demonstration where a forward bias was applied to the thermoelectric devices to return the glove to a soft state (Figure 5e, pink regions).

2.8 Conclusion

In summary, our work introduces a variable stiffness material and uses its glass transition to provide kinesthetic feedback in a wearable haptic device. While numerous technologies exist to engage the kinesthetic sense and there are many materials whose stiffness can be tuned, these two concepts have not previously been combined. In addition to functioning as a wearable haptic device, this textile-thermoplastic composite can be healed in the same manner in which it provides kinesthetic feedback, through heating. While the switching times between states of low and high stiffness are currently quite long for practical use, we believe that they can be decreased by increasing the surface area at the interface of the composite and the thermoelectric devices. It may also be possible to increase the thermal conductivity of the thermoplastic component.[26,27] To increase the

deformability of the entire device, we suggest that thermoelectric devices made of stretchable components would also prove valuable.[28] Some of the variation in response times and bending-stiffness samples can be attributed to the thermoelectric devices used to heat the textile-thermoplastic composite. Thermoelectric devices will continuously increase their temperature over time when held at a particular voltage. In future work, integrating the thermoelectric devices with a thermal sensor and proportional integral derivative (PID) controller would provide the capability of stabilizing the thermoelectric devices at a specified temperature. The field of soft materials may have a significant role in the development of wearable haptic technologies.[29] A similar recognition of the importance of soft materials is already underway in the fields of soft robotics[30] and stretchable electronics.[31–33] Beyond the production of haptic technologies, the science of soft materials may also help accelerate our understanding of the human tactile sense.[34,35] Making progress in these areas provide an exciting platform for interdisciplinary research involving chemistry, materials science, engineering, and cognitive science.

Chapter 2, in full, is a reprint of the material as it appears in Sensors and Actuators A: Physical 2019. Carpenter, C.W.[1], Tan, S.T.M.[1], Keef, C., Skelil, K., Malinao, M., Rodriquez, D., Alkhadra, M.A., Ramírez, J., Lipomi, D.J. The dissertation author was the primary investigator and author of this paper.

2.9 References

[1] J. C. Tuthill, E. Azim, *Curr. Biol.* **2018**, *28*, R194.

[2] A. C. McConnell, M. Vallejo, R. C. Moioli, F. L. Brasil, N. Secciani, M. P. Nemitz, C. P. Riquart, D. W. Corne, P. A. Vargas, A. A. Stokes, *Front. Mech. Eng.* **2017**, *3*, 1.

[3] L. Cappello, J. T. Meyer, K. C. Galloway, J. D. Peisner, R. Granberry, D. A. Wagner, S. Engelhardt, S. Paganoni, C. J. Walsh, *J. NeuronEngineering Rehabil.* **2018**, *15*, 59.

[4] C. Pacchierotti, S. Sinclair, M. Solazzi, A. Frisoli, V. Hayward, D. Prattichizzo, *IEEE Trans. Haptics* **2017**, *10*, 580.

[5] Y. S. Narang, J. J. Vlassak, R. D. Howe, *Adv. Funct. Mater.* **2018**, *28*, 1707136.

[6] S. Jadhav, V. Kannanda, B. Kang, M. T. Tolley, J. P. Schulze, *IS&T Int. Symp. Electron. Imaging 2017* **2017**, 19.

[7] P. Polygerinos, Z. Wang, K. C. Galloway, R. J. Wood, C. J. Walsh, *Rob. Auton. Syst.* **2015**, *73*, 135.

[8] B. H. In, B. B. Kang, M. Sin, K. Cho, *IEEE Robot. Autom. Mag.* **2015**, 97.

[9] R. Rizzo, A. Musolino, L. A. Jones, *IEEE Trans. Haptics* **2018**, *11*, 317.

[10] S. Rich, S. H. Jang, Y. L. Park, C. Majidi, *Adv. Mater. Technol.* **2017**, *2*, 1700179.

[11] I. M. Van Meerbeek, B. C. Mac Murray, J. W. Kim, S. S. Robinson, P. X. Zou, M. N. Silberstein, R. F. Shepherd, *Adv. Mater.* **2016**, *28*, 2801.

[12] M. Solazzi, W. R. Provancher, A. Frisoli, M. Bergamasco, *IEEE World Haptics Conf.* **2011**, 31.

[13] S. M. Felton, K. P. Becker, D. M. Aukes, R. J. Wood, *Soft Matter* **2013**, *9*, 7688.

[14] Y. Liu, B. Shaw, M. D. Dickey, J. Genzer, *Sci. Adv.* **2017**, *3*, 1.

[15] J. Van Humbeeck, *Adv. Eng. Mater.* **2001**, *3*, 837.

[16] G. Strobl, *The Physics of Polymers: Concepts for Understanding Their Structures and Behavior*, **2007**.

[17] T. P. Chenal, J. C. Case, J. Paik, R. K. Kramer, *IEEE Int. Conf. Intell. Robot. Syst.*

2014, 2827.

[18] M. C. Yuen, R. A. Bilodeau, R. K. Kramer, *IEEE Robot. Autom. Lett.* **2016**, *1*, 708.

[19] J. S. Heo, J. Eom, Y.-H. Kim, S. K. Park, *Small* **2017**, *14*, 1.

[20] H. Jin, N. Matsuhisa, S. Lee, M. Abbas, T. Yokota, T. Someya, *Adv. Mater.* **2017**, *29*, 1605848.

[21] L. Zhang, M. Fairbanks, T. L. Andrew, *Adv. Funct. Mater.* **2017**, *27*, 1700415.

[22] Y. Zhao, A. Gumyusenge, J. He, G. Qu, W. W. McNutt, Y. Long, H. Zhang, L. Huang, Y. Diao, J. Mei, *Adv. Funct. Mater.* **2018**, *28*, 1705584.

[23] U. Gaur, S. F. Lau, B. B. Wunderlich, B. Wunderlich, *J. Phys. Chem. Ref. Data* **1982**, *11*, 1065.

[24] J. Richeton, S. Ahzi, K. S. Vecchio, F. C. Jiang, R. R. Adharapurapu, *Int. J. Solids Struct.* **2006**, *43*, 2318.

[25] Y. J. Tan, J. Wu, H. Li, B. C. K. Tee, *ACS Appl. Mater. Interfaces* **2018**, *10*, 15331.

[26] S. Hong, H. Lee, J. Lee, J. Kwon, S. Han, Y. D. Suh, H. Cho, J. Shin, J. Yeo, S. H. Ko, *Adv. Mater.* **2015**, *27*, 4744.

[27] M. D. Bartlett, N. Kazem, M. J. Powell-Palm, X. Huang, W. Sun, J. A. Malen, C. Majidi, *Proc. Natl. Acad. Sci.* **2017**, *114*, 2143.

[28] B. Russ, A. Glaudell, J. J. Urban, M. L. Chabinyc, R. A. Segalman, *Nat. Rev. Mater.* **2016**, *1*, 16050.

[29] M. Ying, A. P. Bonifas, N. Lu, Y. Su, R. Li, H. Cheng, A. Ameen, Y. Huang, J. A. Rogers, *Nanotechnology* **2012**, *23*, 344005.

[30] P. Polygerinos, N. Correll, S. A. Morin, B. Mosadegh, C. D. Onal, K. Petersen, M. Cianchetti, M. T. Tolley, R. F. Shepherd, *Adv. Eng. Mater.* **2017**, *19*, 1700016.

[31] M. L. Hammock, A. Chortos, B. C. K. Tee, J. B. H. Tok, Z. Bao, *Adv. Mater.* **2013**, *25*, 5997.

[32] J. H. Koo, D. C. Kim, H. J. Shim, T. H. Kim, D. H. Kim, *Adv. Funct. Mater.* **2018**, *1801834*, 1.

[33] J. Wang, M. F. Lin, S. Park, P. S. Lee, *Mater. Today* **2018**, *21*, 508.

[34] L. Skedung, M. Arvidsson, J. Y. Chung, C. M. Stafford, B. Berglund, M. W. Rutland, *Sci. Rep.* **2013**, *3*, 2617.

[35] C. W. Carpenter, C. Dhong, N. B. Root, D. Rodriquez, E. E. Abdo, K. Skelil, M. A. Alkhadra, J. Ramírez, V. S. Ramachandran, D. J. Lipomi, *Mater. Horizons* **2018**, *5*, 70.

3 Ionotactile Stimulation: Nonvolatile Ionic Gels for Human-Machine Interfaces

*ACS Omega 2018

3.1 Abstract

We report the application of a nonvolatile ionic gel as a soft, conductive interface for electrotactile stimulation. Materials characterization, and psychophysical experiments reveal that a glycerol-containing ionic gel exhibits better stability in air, improved adhesive properties, and a wider window of comfortable stimulation when compared to a conventional aqueous ionic hydrogel.

3.2 Introduction

The skin is the body's largest organ.[1] It is equipped with a variety of sensing functionalities with which electronic devices can be interfaced to transmit information to the brain. The tactile sense, thus, provides a natural route for augmenting human-machine interactions. Electrotactile stimulation is one way for information to be communicated through the skin—in the form of a locally resolved tingling sensation.[2] Conventional electrotactile devices use metallic conductors to couple capacitively with ions in cutaneous tissue, activate nerve afferents, and manifest as a sensation of touch. In this report, we introduce a new concept: the use of a nonvolatile, ionically conductive gel as a soft interface between the rigid electronic circuitry of machines, and the natural ionic circuitry of humans (**Figure 1**).

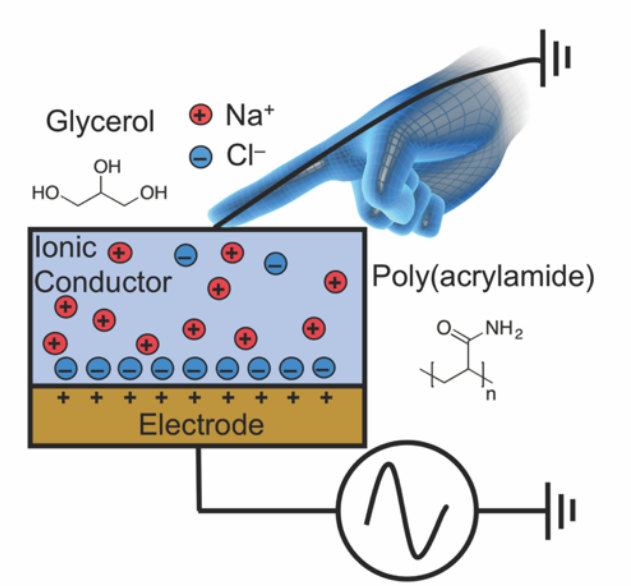

Figure 1. Schematic diagram illustrating the concept of an ionotactile device in a monopolar stimulation configuration. A soft and deformable ionic conductor is used as an interface between a metallic electrode and human skin.

The rapidly advancing field of stretchable electronics is changing the way devices are designed—especially those meant to interface with humans.[3,4] Architectures for electrotactile devices have evolved accordingly. Originally designed using conventional electronic materials, electrotactile devices were restricted to rigid surfaces.[2] Such devices were explored for programmable braille readers and displays for the visually impaired.[5] More recently, advances in fabrication methods have enabled the development of conformable devices that use geometrically patterned electronic conductors on the surface of elastomers to improve the interface for electrotactile stimulation.[6,7] Such devices make use of materials that are not intrinsically soft and thus require advanced fabrication techniques to pattern into serpentine structures that can withstand strain and conform to the skin.

Ionic hydrogels have concurrently emerged as promising conductors for a variety of sensing and actuation applications due to their optical transparency, mechanical softness,

biocompatibility, and capacity to self-heal.[8–10] This unique combination of properties has enabled the development of several novel applications including transparent loudspeakers,[11] wearable sensors,[12–14] underwater microphones,[15] and electroluminescent devices.[16,17] Furthermore, these materials can be 3D printed,[18,19] and chemically bonded to diverse surfaces,[20,21] enabling cheap, rapid, and precise manufacturing of robust devices. Such creative demonstrations have inspired us to consider this class of materials as potentially useful for providing electrotactile stimulation as part of a soft haptic device.

3.3 Results and Discussion

As a first demonstration, we used a standard poly(acrylamide) (PAAm) hydrogel containing an aqueous sodium chloride solution. The modulus of PAAm is commensurate with that of biological tissue (~10 kPa), biocompatible, and with which it is possible to fabricate objects in well-defined geometries using 3D printing techniques.[18,19] A function generator was used to pass a biphasic square wave alternating current through the hydrogel into the index finger of a subject. Upon contacting the hydrogel with an electrically grounded finger in a monopolar configuration,[22] a mild tingling sensation was perceived. As the force applied by the finger was increased, the sensation grew stronger.

Evaporation of water from the ionic hydrogel is a particularly important obstacle in this application because the device geometry requires that the hydrogel be exposed to air, and thus encapsulation is not viable. Ionic liquids[23] and highly hydratable salts such as lithium chloride[24] have been proposed as strategies to mitigate drying, however, these liquids are acutely toxic and thus cannot be used in place of salt water for this application. To overcome this constraint, we replaced the salt water with a solution of glycerol containing 0.7 M NaCl. Glycerol is a biocompatible, low-vapor pressure fluid (T_B = 290

°C) that is capable of dissolving ions, albeit at lower concentrations than water. Replacement of the water was achieved by simply soaking a hydrated hydrogel in a glycerol solution overnight. This process led to an observable shrinkage of the gel; a ~60% reduction in volume was measured using calipers. Mass-loss experiments, shown in **Figure 2a**, revealed that the replacement of water with the glycerol solution resulted in a conductive gel that was stable in air. While the water rapidly evaporated from the aqueous hydrogel under ambient conditions with a mass decay time of approximately 10 h, the glycerol gel absorbed some moisture from the air to increase its mass slightly before reaching equilibrium. Due to the hydroscopic nature of glycerol, it can be expected that fluctuations in the relative humidity of the environment will lead to minor changes in the equilibrium concentration of water in the gel.

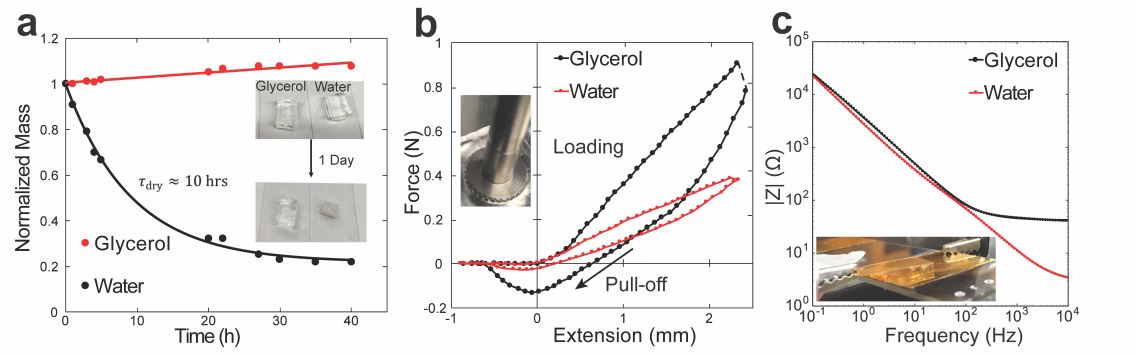

Figure 2. Materials Characterization. (a) Normalized mass as a function of time under ambient conditions demonstrating the stability of the ionic glycerol gel in air. Insets show photographs of gels before and after experiments. (b) Indentation and pull-off curves obtained using the cylindrical stainless steel punch shown in the inset. (c) Electrochemical impedance spectra obtained using the parallel plate capacitor geometry shown in the inset.

In handling the two materials, we observed that the glycerol gel exhibited stronger adhesion to the finger than the hydrogel. Such adhesive properties are desirable for maintaining a stable interface with the user's skin during use of a device. To compare the adhesive and mechanical properties of these two materials, we performed mechanical

indentation experiments on rectangular slabs using a stainless steel cylindrical punch. As shown in **Figure 2b**, we found that the glycerol gel exhibited both a stiffer response to indentation, as well as a significantly stronger pull-off force. The elastic modulus was extracted from these curves using an appropriate model[25] to correct for the finite thickness of the hydrogel sample (see **Supplementary Information, Section 2**). We found that the aqueous ionic hydrogel had a compressive elastic modulus of 27 kPa while the glycerol gel had a higher value of 80 kPa. This increase in stiffness was consistent with the observed shrinkage of the gel upon replacing water with glycerol. Moreover, the pull-off force for the glycerol gel was a full order of magnitude larger than the hydrogel, in agreement with our qualitative observation of an improved adhesive interface with the skin.

It was expected that the replacement of water with glycerol would increase the electrical impedance due to a lower concentration of ions, and higher viscosity. Electrochemical impedance spectroscopy was used to characterize the electrical response of the two materials. Gold electrodes, sputtered onto flexible poly (ethylene terephthalate) (PET) films, were used as blocking electrodes in a parallel plate capacitor geometry (1 cm × 1 cm × 0.2 cm). **Figure 2c** shows the measured impedance spectrum. The glycerol gel exhibited a slightly higher impedance over the frequency range relevant for electrotactile stimulation (1-1000 Hz), however, order-of-magnitude differences only occur at frequencies over 1000 Hz, suggesting that these two materials should behave comparably in ionotactile devices. A more detailed analysis of the impedance data using equivalent circuit modeling is given in **Section 3** of the **Supplementary Information**, this analysis revealed that the series resistance of the glycerol gel was approximately an order of magnitude greater than the ionic hydrogel.

To determine sensation threshold curves, a simple finger stimulator device was fabricated using a mold-casting process described in the **Supplementary Information, Section 5**. Ecoflex® 00-30 was used as the housing material (**Figure 3a**), and the ionic gel was addressed using a film of PET containing a film of sputtered gold. We note here that over the course of our electrical stimulation experiments we did not observe any changes in the appearance or electrical properties of the device, indicating that no irreversible electrochemical reactions occurred at the electrode interface. Magnets embedded within the Ecoflex® were used to attach the device to the user's finger. We tested the device performance using simple psychophysical experiments on a pool of four subjects. Experiments were performed using a "free-exploration" approach, where the subject manually adjusted the voltage until they perceived a sensation, corresponding to the lower bound for tactile stimulation. Once a lower bound was determined, subjects increased the voltage until they felt like the sensation would no longer be considered comfortable to determine an upper bound. A wide range of frequencies were tested to construct the sensation curves shown in **Figure 3b, c**.

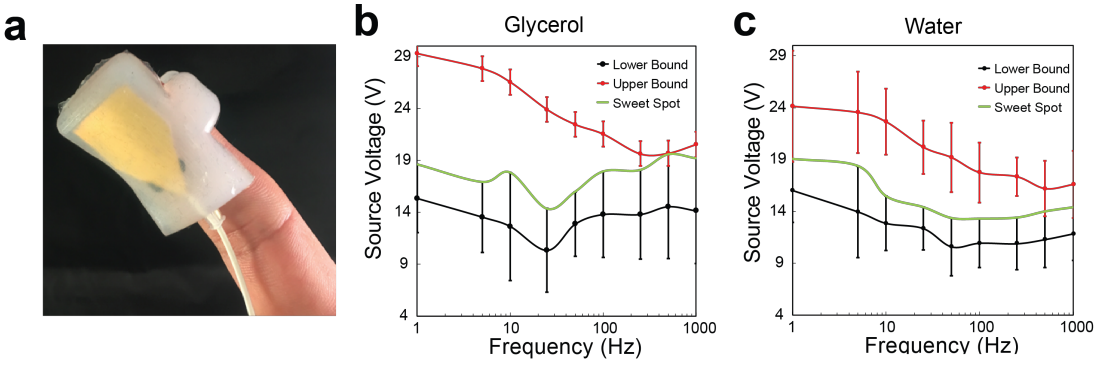

Figure 3. Ionotactile device characterization. (a) Image of device worn on the index finger. Sensation curves showing the source voltage required for stimulation for a range of frequencies for (b) glycerol and (c) water. Error bars show the standard deviation between four subjects.

In agreement with our impedance measurements, we found that the glycerol gel exhibited comparable performance to the hydrogel when incorporated into the device. For both materials, subjects observed that below 10 Hz individual pulsations were discernable, while above 10 Hz only a continuous tingling sensation was perceived. Such experiments are inherently subjective, and therefore the observed variance across subjects was not surprising. Interestingly, we found that, in the range of 1-100 Hz, the glycerol gel had a larger window of comfortable stimulation. For both materials, we constructed a voltage-frequency curve that corresponds to a "sweet spot" for comfortable stimulation that would be perceptible to all users. This was obtained by simply adding the standard deviation to the average of the lower bound for stimulation.

To demonstrate pixelation of the ionic gel, the device shown in **Figure 4** was fabricated. The electrodes were designed such that the middle pixel was a common ground, while the upper and lower pixels applied the stimulating voltage, corresponding to a bipolar electrode configuration.[26] Films of Mylar® (aluminum-coated PET films) were used to electrically address the pixels. With this design, we found that the two stimulating pixels could be distinguished by the user; this experiment demonstrated that spatial resolution was possible. We also found that the threshold voltage for sensation was significantly higher: approximately 80 V at 50 Hz. We expect that the use of 3D printing technology to pattern the electrodes into a concentric design comprising an inner disk and outer ring[6] would facilitate more localized tactile sensations at a lower stimulating voltage. Finally, it is important to note that humans naturally integrate visual and haptic signals in an optimal fashion.[27] Therefore a wider range of tactile sensations could be accessible when such a device is paired with visual stimuli.

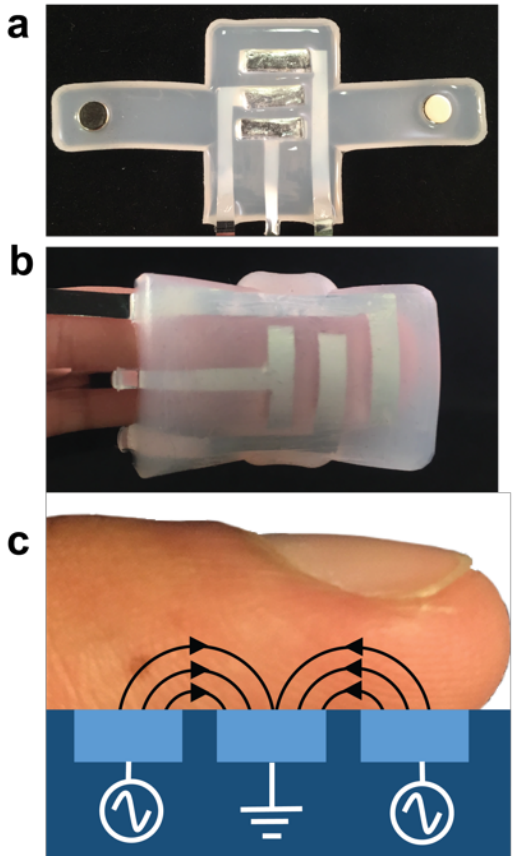

Figure 4. Pixelated ionotactile device. (a) Top-down view of device. The middle electrode is the common ground, while the top and bottom electrodes are stimulating pixels. (b) Device worn on a finger. (c) Schematic diagram showing the electric field lines associated with a bipolar stimulation geometry.

3.4 Conclusions

We have developed a nonvolatile, transparent, ion-conducting gel to demonstrate an innovation in haptic technology: an ionotactile device. This device enables an improved route for human-machine interaction and has potential to be integrated with emerging technologies such as virtual and augmented reality. We found that the use of a saline glycerol PAAm gel was superior to a conventional ionic hydrogel due to stability in air, improved adhesion with the user, and a larger window for comfortable electrical stimulation in the range of 1-100 Hz. One potential extension of this technology would be

to create a multi-modal device that is capable of simultaneously sensing mechanical deformations[12] and responding by sending a haptic signal to the user. This multi-modal functionality in conjunction with tissue-like mechanical properties make the ionic gel a particularly attractive material for robot-assisted telesurgery applications.[28]

Chapter 3, in full, is a reprint of the material as it appears in ACS Omega 2018. Root, S.E., Carpenter, C.W., Kayser, L.V., Rodriquez, D., Davies, D.M., Wang, S., Siew Tan, S.T.M., Meng, Y.S., Lipomi, D.J. The dissertation author was the secondary investigator and author of this material.

3.5 References

[1] McGrath, J. A.; Uitto, J. Anatomy and Organization of Human Skin. In *Rook's Textbook of Dermatology, Eighth Edition*; Blackwell Publishing: New Jersey, 2010.

[2] Kajimoto, H.; Kawakami, N.; Maeda, T.; Tachi, S. Electro-Tactile Display with Tactile Primary Color Approach. *Proc. Int. Conf. Intell. Robot. Syst.* **2004**, *10*, 1–13.

[3] Wang, H.; Ma, X.; Hao, Y. Electronic Devices for Human-Machine Interfaces. *Adv. Mater. Interfaces* **2017**, *4*, 1–20.

[4] Kim, J.; Lee, M.; Shim, H. J.; Ghaffari, R.; Cho, H. R.; Son, D.; Jung, Y. H.; Soh, M.; Choi, C.; Jung, S.; *et al.* Stretchable Silicon Nanoribbon Electronics for Skin Prosthesis. *Nat. Commun.* **2014**, *5*, 1–11.

[5] Bach-y-rita, P.; Tyler, M. E.; Kaczmarek, K. A. Seeing with the Brain. *Int. J. Hum. Comput. Interact.* **2003**, *15*, 285–295.

[6] Ying, M.; Bonifas, A. P.; Lu, N.; Su, Y.; Li, R.; Cheng, H.; Ameen, A.; Huang, Y.; Rogers, J. a. Silicon Nanomembranes for Fingertip Electronics. *Nanotechnology* **2012**, *23*, 1–7.

[7] Lim, S.; Son, D.; Kim, J.; Lee, Y. B.; Song, J. K.; Choi, S.; Lee, D. J.; Kim, J. H.; Lee, M.; Hyeon, T.; *et al.* Transparent and Stretchable Interactive Human Machine Interface Based on Patterned Graphene Heterostructures. *Adv. Funct. Mater.* **2015**, *25*, 375–383.

[8] Keplinger, C.; Sun, J.-Y.; Foo, C. C.; Rothemund, P.; Whitesides, G. M.; Suo, Z. Stretchable, Transparent, Ionic Conductors. *Science.* **2013**, *341*, 984–987.

[9] Rogers, J. A. A Clear Advance in Soft Actuators. *Science.* **2013**, *341*, 968–970.

[10] Cao, Y.; Morrissey, T. G.; Acome, E.; Allec, S. I.; Wong, B. M.; Keplinger, C.; Wang, C. A Transparent, Self-Healing, Highly Stretchable Ionic Conductor. *Adv. Mater.* **2017**, *29*.

[11] Keplinger, C.; Sun, J.; Foo, C. C.; Rothemund, P.; Whitesides, G. M.; Suo, Z. Stretchable, Transparent, Ionic Conductors. *Science.* **2013**, *341*, 984–987.

[12] Sun, J. Y.; Keplinger, C.; Whitesides, G. M.; Suo, Z. Ionic Skin. *Adv. Mater.* **2014**, *26*, 7608–7614.

[13] Kim, C.-C.; Lee, H.-H.; Oh, K. H.; Sun, J.-Y. Highly Stretchable, Transparent Ionic Touch Panel. *Science.* **2016**, *353*, 682–687.

[14] Sarwar, M. S.; Dobashi, Y.; Preston, C.; Wyss, J. K. M.; Mirabbasi, S.; David, J.; Madden, W. Bend , Stretch , and Touch : Locating a Finger on an Actively Deformed Transparent Sensor Array. *Sci. Adv.* **2017**, *3*, 1–9.

[15] Gao, Y.; Song, J.; Li, S.; Elowsky, C.; Zhou, Y.; Ducharme, S.; Chen, Y. M.; Zhou, Q.; Tan, L. Hydrogel Microphones for Stealthy Underwater Listening. *Nat. Commun.* **2016**, *7*, 1–10.

[16] Yang, C. H.; Chen, B. H.; Zhou, J. X.; Chen, Y. M.; Suo, Z. G. Electroluminescence of Giant Stretchability. *Adv. Mater.* **2016**, *28*, 4480–4484.

[17] Larson, C.; Peele, B.; Li, S.; Robinson, S.; Totaro, M.; Beccai, L.; Mazzolai, B.; Shepherd, R.; Barbosa, A.; Allen, J. J.; *et al.* Highly Stretchable Electroluminescent Skin for Optical Signaling and Tactile Sensing. *Science.* **2016**, *351*, 1071–1074.

[18] Barry, R. A.; Shepherd, R. F.; Hanson, J. N.; Nuzzo, R. G.; Wiltzius, P.; Lewis, J. A. Direct-Write Assembly of 3D Hydrogel Scaffolds for Guided Cell Growth. *Adv. Mater.* **2009**, *21*, 2407–2410.

[19] Tian, K.; Bae, J.; Bakarich, S. E.; Yang, C.; Gately, R. D.; Spinks, G. M.; in het Panhuis, M.; Suo, Z.; Vlassak, J. J. 3D Printing of Transparent and Conductive Heterogeneous Hydrogel-Elastomer Systems. *Adv. Mater.* **2017**, 1604827.

[20] Yuk, H.; Zhang, T.; Lin, S.; Parada, G. A.; Zhao, X. Tough Bonding of Hydrogels to Diverse Non-Porous Surfaces. *Nat. Mater.* **2015**, *15*, 190–196.

[21] Yuk, H.; Zhang, T.; Parada, G. A.; Liu, X.; Zhao, X. Skin-Inspired Hydrogel–elastomer Hybrids with Robust Interfaces and Functional Microstructures. *Nat. Commun.* **2016**, *7*, 1–11.

[22] Merrill, D. R.; Bikson, M.; Jefferys, J. G. R. Electrical Stimulation of Excitable Tissue: Design of Efficacious and Safe Protocols. *J. Neurosci. Methods* **2005**, *141*, 171–198.

[23] Chen, B.; Lu, J. J.; Yang, C. H.; Yang, J. H.; Zhou, J.; Chen, Y. M.; Suo, Z. Highly Stretchable and Transparent Ionogels as Nonvolatile Conductors for Dielectric Elastomer Transducers. *ACS Appl. Mater. Interfaces* **2014**, *6*, 7840–7845.

[24] Bai, Y.; Chen, B.; Xiang, F.; Zhou, J.; Wang, H.; Suo, Z. Transparent Hydrogel with Enhanced Water Retention Capacity by Introducing Highly Hydratable Salt. *Appl. Phys. Lett.* **2014**, *1-5*.

[25] Shull, K. R.; Ahn, D.; Chen, W.-L.; Flanigan, C. M.; Crosby, A. J. Axisymmetric Adhesion Tests of Soft Materials. *Macromol. Chem. Phys.* **1998**, *199*, 489–511.

[26] Comte, P. Monopolar versus Bipolar Stimulation. *Proc. 8th Meet. World Soc. Stereotact. Funct. Neurosurgery, Part I* **1981**, *45*, 156–159.

[27] Ernst, M. O.; Banks, M. S. Humans Integrate Visual and Haptic Information in a Statistically Optimal Fashion. *Nature* **2002**, *415*, 429–433.

[28] Marescaux, J.; Leroy, J.; Gagner, M.; Rubino, F.; Mutter, D.; Vix, M.; Butner, S. E.; Smith, M. K. Transatlantic Robot-Assisted Telesurgery. *Nature* **2001**, *413*, 379–380.

4 Electropneumotactile Stimulation: Multimodal Haptic Actuator Enabled by Stretchable Conductive Polymer on Inflatable Blisters

4.1 Abstract

Recapitulating the sense of touch in a virtual environment requires technologies that stimulate receptors beneath the skin. Haptic devices—technologies designed to interact with the sense of touch—ideally deliver multiple sensations to the skin at the same time. Here, we introduce a multimodal haptic actuator—an "electropneumotactile" device—that delivers both mechanical and electrical stimulation simultaneously. Mechanical stimulation is delivered by a silicone-based pneumatic actuator while the electrical stimulation is delivered by a stretchable conductive polymer blend of poly(3,4-ethylenedioxythiophene) (PEDOT) and polyurethane (PU). The blend of PEDOT and PU has a 146 MPa modulus and remains conductive following out-of-plane cyclic loading (100 cycles) at a rate of 330 mm/min. The stretchability of both components allows for the electrotactile stimulator to be superimposed upon the pneumatic stimulator and for dual delivery of two sensations to the same location on the skin. These results are confirmed by way of human subject experiments that show subjects can successfully detect the location of pneumatic stimulation and whether electrotactile stimulation is delivered (yes/no) at a rate above chance (mean accuracy = 94%).

4.2 Introduction

The ability to simulate complex tactile sensations in a wearable haptic device in

virtual and augmented reality (VR and AR) depends on co-location of the active components. That is, tactile "pixels" that are capable of more than one type of stimulation at the same time (much like a pixel in a display contains red, green, and blue subpixels). In this paper, we use a stretchable conductive polymer to enable simultaneous mechanical and electrical stimulation in the same location on the skin through a device which we refer to as an "electropneumotactile" actuator (Figure 1). Specifically, we used inflatable pockets (blisters) in elastomeric slabs overlaid with patterned electrodes made of a conductive polymer. Critically, the polymer was engineered to withstand repeated inflation of the blisters in the substrate. A pneumatic—"pneumotactile"—device produces deflections with displacements of ≥100 μm,[1] which are perceived as a bumpy topography or vibration of a virtual object, depending on whether or not the state of inflation is static or periodic. In contrast, the electrical—electrotactile—modality can be made to feel tingly or to mimic (roughly) the fine texture of surfaces. This study describes the use of the conducting polymer poly(3,4-ethylenedioxythiophene) (PEDOT) as a stretchable electrotactile stimulator in conjunction with a pneumatic actuator. This arrangement enables multimodal haptic sensations, as demonstrated in human subject experiments. We chose PEDOT as the electrode material due to its ease of processing, biocompatibility, and tunable electrical and mechanical properties. Specifically, we chose a PEDOT:tosylate (PEDOT:OTs) polymer blend with polyurethane (PU), Figure 1 (inset), which we call "PEDOT/PU" throughout the paper.[2]

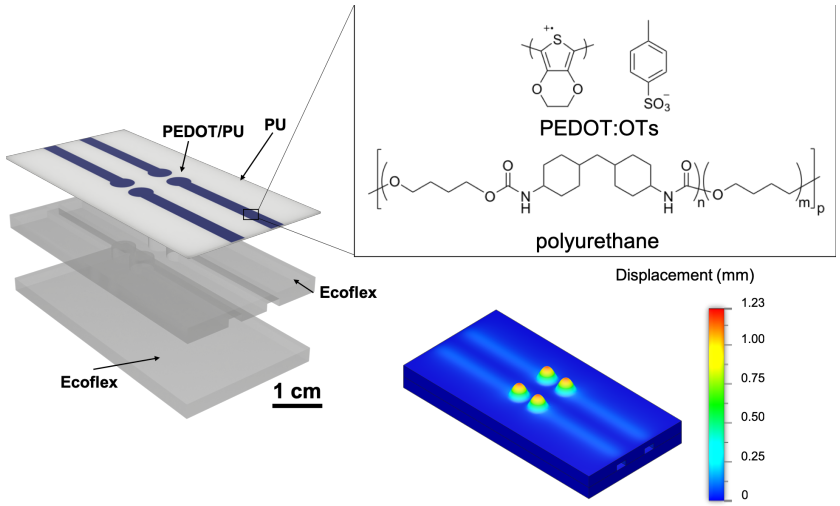

Figure 1. Schematic drawing of a multimodal haptic actuator comprising stretchable electrotactile stimulators (PEDOT/PU) superimposed on pneumatic actuators (Ecoflex). (Inset) chemical structures of ethylenedioxythiophene with tosylate and polyurethane (PU). (Bottom) Finite element analysis of 4 pneumatic pixels used to simulate the magnitude of displacement of each blister when "inflated." The channels are composed of 0.15 MPa Ecoflex and a 1 N force was applied to the internal walls of each pneumatic channel.

4.3 Background

Multimodal haptic actuators are crucial for enriching tactile and kinesthetic sensations in commercial virtual and augmented reality systems. There are three general approaches for delivering multiple sensations to the skin. Different approaches have been taken to deliver multiple sensations. Some of these approaches include a combination of DC motors and electrotactile stimulators for mechanical and electrical stimulation,[3] electrostatic and vibrotactile stimulators for variable-friction and vibrational surfaces, and thermal and vibrotactile stimulators for temperature and vibrational feedback.[4] Two forms of haptic stimulation that have not been previously combined are pneumatic stimulators and electrotactile stimulators. Ideally these stimulators are directly upon one another so that both mechanical and electrical sensations could be delivered to the same location. The inability to combine these two forms of stimulation can be attributed to mismatch in

mechanical properties between the elastomeric materials used in pneumatic actuators and the metallic materials used in electrotactile stimulators. Pneumatic actuators stimulate the sense of touch through the inflation of elastomeric "blisters" upon inflation. Metallic electrodes on the surface of an underlying elastomeric-pneumatic actuator would be difficult or impossible because of the likelihood of fracture upon inflation of the blisters.

Pneumatic actuators can be arranged into pixelated arrays for refreshable-Braille displays.[5] The body of a pneumatic actuator is typically fabricated using silicone based elastomeric materials such as poly(dimethylsiloxane) and Ecoflex.[5,6] Soule and Lazarus demonstrated a silicone based refreshable Braille device which could be "locked" into place by filling the pockets with low-melting metals for Braille-based street signs for the blind.[5] The advantage of pixels which lock in place is that they do not require power in the "off-state," similar to e-ink pixels found in modern reading devices. Besse et al. fabricated a refreshable-Braille display with a matrix of 32 × 24 pixels made of a shape memory polymer. Individual pixels were selectively heated by stretchable heaters and then actuated with a single valve-supply of air.[7] Kwon et al. filled pneumatic pockets with fluid which expanded when heated by a resistive heating wire.[6] The advantage of thermal expansion as opposed to inflation is that it does not need channels to deliver air to each blister individually, nor large device components such as compressed air tanks and control valves. In another approach, Qiu et al. used a bistable electroactive polymer to deflect a rigid pin into the skin.[8] While these devices are novel forms of refreshable-Braille devices they all deliver a single mechanical-mode of stimulation.

Electrotactile stimulation is a form of sensory substitution that uses an alternating current (~2-4 mA) to stimulate nerve endings in the skin.[9] Electrotactile stimulators rely

on capacitive coupling between an electrical conductor and ions in sweat to excite mechanoreceptors (neurons responsible for detecting mechanical forces) and nociceptors (responsible for signaling pain) in the skin. Electrotactile stimulators are used as sensory substitution systems for the blind,[10,11] as feedback within prosthetic limbs for amputees,[12–14] as well as muscle stimulators to reduce pain non-invasively.[15] Early forms of electrotactile stimulators were made out of bulky, rigid metals, which do not conform easily to the curved and deformable surface of the skin. More recently, devices of thin Ag/AgCl electrodes coated with conductive gels have enabled electrotactile stimulators to be flexible.[12–14] Ying et al. demonstrated a wearable electrotactile device using serpentine patterned gold electrodes on the inner surface of an Ecoflex "thimble."[16] The thimble had six electrodes for stimulation that could be activated individually. Although the thimble used gold as the electrode material, the device achieved stretchability through the unwinding of serpentine structures. Lim et al. have shown that 2D materials such as graphene may also serve as wearable electrotactile devices.[17] In their study, graphene heterostructures served as the electrode material and exhibited a large degree of conformability to the skin. While both materials accommodate out-of-plane bending due to their thinness, neither can withstand the mechanical strains exerted by a pneumatic actuator blister. Ionic gels containing glycerol and water have also proven to be effective in generating electrotactile stimulation.[18] These gels offer more desirable mechanical properties including low moduli and high toughness. Unlike their "dry" material counterparts where ions are supplied by sweat from the skin, ionic gels supply additional ions suspended in solution within the material itself. Ions incorporated in the gel capacitively couple with thin-film gold electrodes located beneath the device. While ionic

gels exhibit the ability to withstand the strains produced by pneumatic actuators, the underlying gold electrodes cannot. The inability of electrotactile stimulators to combine with pneumatic actuators calls for new materials that are both mechanically compliant and electrically conductive.

In their native state, conductive polymers are nearly as brittle as work-hardened metals.[19] The mechanical stiffness of conductive polymers can be reduced while maintaining sufficient conductivity by the use of additives or covalent modifications to the polymer. For example, the stretchability of PEDOT:PSS may be increased by the addition of surfactants such as Capstone and Triton X-100,[20] by blending with elastomers such as polyurethane[2] (used in this study), or through chemical modification of the backbone.[19,21] The conductivity of PEDOT:PSS can be improved by addition of high-boiling point solvents, such as dimethyl sulfoxide and ethylene glycol.[19] These high-boiling point solvents also have the effect of plasticizing PEDOT:PSS, allowing films to accommodate ≥50% strain. PEDOT:PSS, when used as a surface coating, can also reduce the electrochemical impedance of metallic electrodes used to record and stimulate neurons.[22–25] The 3D structure of PEDOT:PSS gives coated metallic electrodes the property of reduced impedance due to an increase in the number of ions that capacitively couple at the electrode-electrolyte interface compared to an uncoated metallic electrode.

4.4 Results and Discussion

4.4.1 Electropneumotactile design and fabrication

The stretchable electrotactile and pneumatic actuators were combined using the fabrication scheme depicted in Figure 2. The electropneumotactile device comprised four PEDOT/PU electrodes supported on a PU substrate and four pneumatic pixels made of Ecoflex. The electrodes were patterned by spray coating a 10 μm layer of PEDOT/PU through a polyimide (PI) mask on glass while heating on a hotplate at 65 °C (steps 1 – 2). After heating for 5 min, the solution transitioned from a translucent yellow to an opaque blue once the EDOT fully polymerized into PEDOT and excess solvents were driven off. Next, the sample was submerged in boiling DI water for 2 s and then in room temperature (22 °C) DI water to remove iron (not pictured). The PI mask was then removed (step 3). The exposed electrodes were then coated with a thin layer of PU dissolved in THF. The sample was kept in a fume hood for 10 h to allow the THF to evaporate and the PU film (~ 0.5 mm thick) to form (step 4). After the film formed, the PU was slowly peeled off of the glass substrate along with the PEDOT/PU electrodes (step 5). In parallel to the PEDOT/PU electrode fabrication, the pneumatic channels and inflatable blisters were fabricated by pouring Ecoflex prepolymer into a 3D-printed mold (step 6). The same step was repeated for the un-patterned base. Both the base and patterned-top layers were then removed from their respective molds (step 7). The base layer, pneumatic top layer, and PEDOT/PU on a PU substrate were adhered to one another by applying a thin coat of Ecoflex prepolymer between the three layers (step 8).

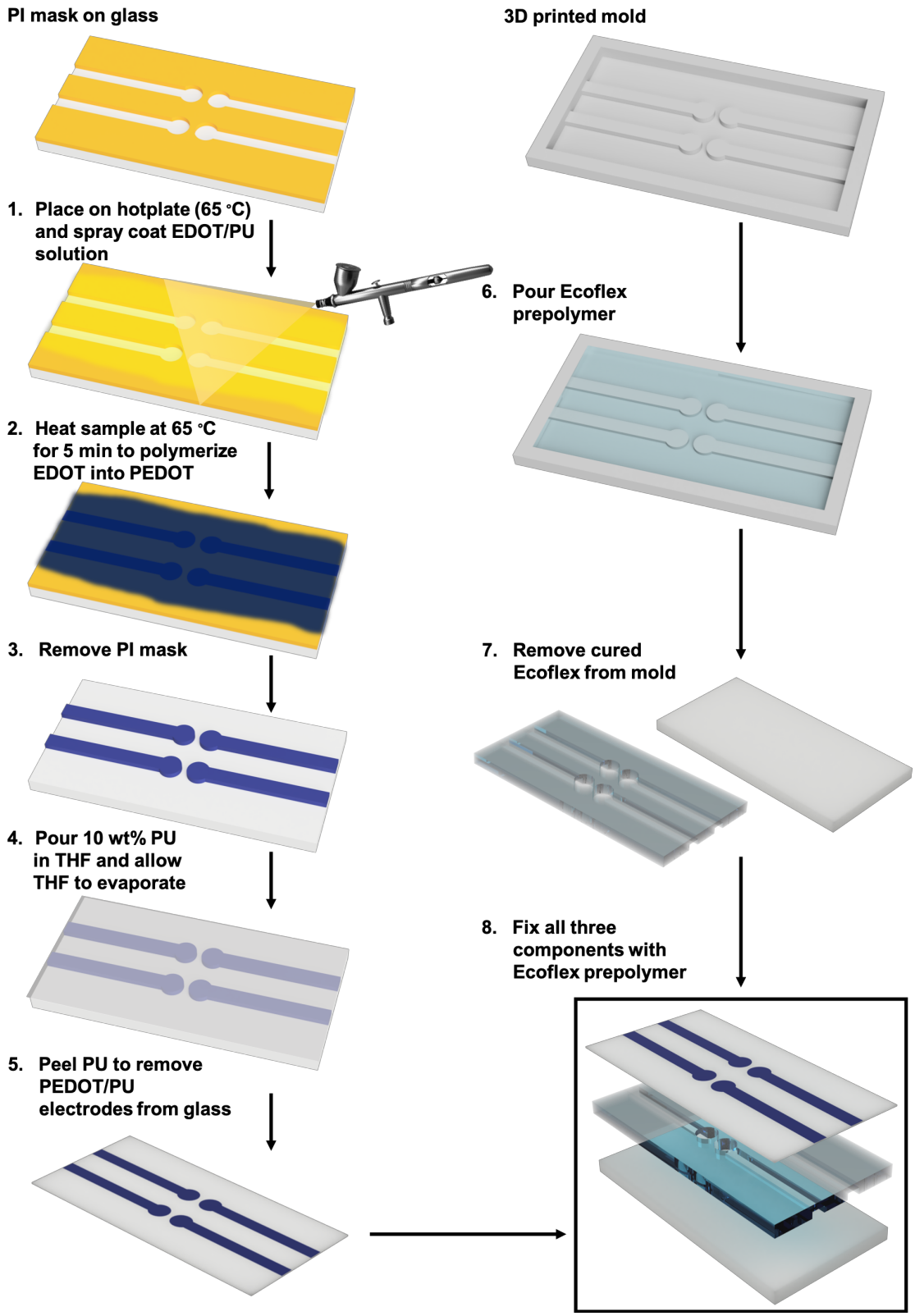

Figure 2. Schematic summarizing the fabrication process of the electropneumotactile device.

4.4.2 Mechanical and electrical characterization of the electropneumotactile device

We performed mechanical and electrical experiments on PEDOT/PU to determine how the electrodes would perform on top of inflated pneumatic blisters. Figure 3a shows the results of a uniaxial pull test of a 1 μm thick layer of PEDOT/PU using the film-on-water technique.[26–28] The thickness of the PEDOT/PU film used to calculate the stress was obtained using a scanning electron microscope (Figure S1). The modulus of PEDOT/PU was 146 MPa and the film fractured at 8% strain. We performed the same test for two other formulations of PEDOT/PU which contained half and a quarter of the PU content by mass (Figure S2). As expected, the blend showed a decrease in modulus as the PU content was increased. The strain at fracture also increased when the PU content was increased.

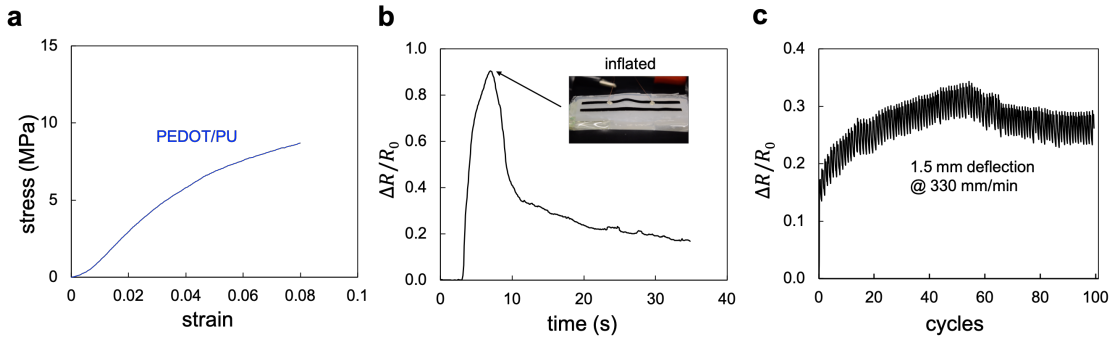

Figure 3. Electromechanical characterization of PEDOT/PU electrodes. (a) Stress-strain analysis of PEDOT/PU. Mechanical testing of thin-films was performed using the film-on-water technique.[26–28] (b) Normalized change in resistance of PEDOT/PU during a single cycle of inflation. (c) Normalized change in resistance of PEDOT/PU on a PU substrate during cyclic loading.

Next, we measured the change in electrical properties of PEDOT/PU when a pneumatic blister was inflated. Figure 3b shows that the resistance of PEDOT/PU increased by approximately 90% when the pneumatic channel is filled. Figure 3b also shows that the

resistance of PEDOT/PU recovered to 15% above its baseline value. The device used in this experiment used modified electrodes (non-pixelated) to properly measure the resistance. Measuring the resistance of a pixelated device would be difficult because the silver paste and copper wire used to make contact would prevent inflation and would likely delaminate from the PEDOT/PU when strained.

Pneumatic actuators are expected to undergo many cycles of inflation when used as a haptic device, therefore, we measured the electrical properties of a PEDOT/PU electrode under cyclic strain. Figure 3c shows the change in resistance of PEDOT/PU on a PU substrate as it was strained 1.5 mm out-of-plane at a rate of 330 mm/min for 100 cycles. The resistance oscillated between ~20% and ~35% above the initial resistance as the PEDOT/PU film was deformed out-of-plane.

4.4.3 Tactile perception & stimulation design

To understand the baseline performance of PEDOT/PU as an electrotactile stimulator in its unstrained state, we conducted a series of human subject experiments. Figure 4a (left) shows the experimental setup used to measure human subjects' sensitivity to electrotactile stimulation. A function generator was used to generate an electrical signal—cathodic first, biphasic square wave with a 50% duty cycle (i.e., net-zero direct current)[9]—which was passed through a linear amplifier that multiplied the signal 20×. A ground electrode was positioned on the palm (on the muscle at the base of the thumb) of the subject. The subjects made contact with a thin-film of PEDOT/PU on glass with their fingertips. Under their own control, subjects increased the voltage by 2 V increments and reported when they felt a slight tingling in their fingertip. The minimum voltage required

to induce a tingling sensation was reported for frequencies between 1 Hz and 1000 Hz (Figure 4a, left). The voltage required for stimulation significantly decreased as the frequency increased from 1 Hz to 100 Hz and begins to level out between 100 Hz and 1 kHz. The voltage required for stimulation is initially high and then drops due to a skin capacitance affect.

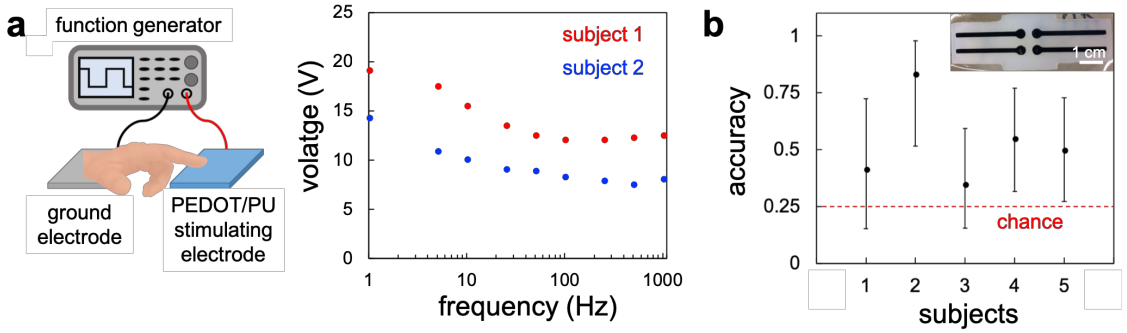

Figure 4. Psychophysical characterization of PEDOT/PU electrodes. (a, Left) Physical setup used to deliver controlled electrotactile stimulation to the fingertip including a function generator to deliver alternating current (charge-balanced, biphasic, square wave) between an electrode on the palm and a thin film of PEDOT/PU on a glass substrate. (a, Right) Individual human subject responses to the minimum voltage required to induce a sensation at a particular frequency. (b) Individual subject accuracy when discriminating between four electrotactile pixels. Error bars are 95% confidence intervals (Clopper-Pearson method for exact binomial confidence intervals). The red dotted line depicts chance performance (25% accuracy). (Inset) Four electrotactile pixels on an electropneumotactile device used to deliver stimulation to the fingertip of a subject.

The manner in which electrotactile electrodes are arranged can affect the voltage required to induce stimulation as well as the resolution. There are two possible configurations of electrodes: monopolar and bipolar. In our experiments, a monopolar configuration was chosen because it requires a lower voltage to induce stimulation.[9] A monopolar configuration has a large separation distance between the stimulating electrode and the ground electrode, while a bipolar electrode configuration places each electrode closer to one another. Bipolar designs can lead to better spatial resolution but require large

stimulating voltages. Monopolar stimulation requires lower voltages but leads to a loss in spatial resolution. The lower voltage requirement observed in monopolar configuration manifests from electric field lines reaching deeper beneath the skin and interacting more strongly with nerves.

Figure 4b shows a 2×2 array of PEDOT/PU electrotactile stimulators and the results of five subjects' accuracy when identifying the location of stimulation. In this experiment, subjects were blindfolded and asked to identify the location of electrotactile stimulation. The same monopolar electrode configuration used in Figure 4a and electrical signal (100 Hz) were used this experiment. The experiment began by calibrating the voltage supplied to each pixel. The calibration step was necessary to ensure that sufficient current (~0.4-0.5 mA) was delivered by each pixel to the fingertip. We used the maximum voltage of the four pixels when administering the accuracy test. Following the calibration step, subjects were asked to identify the position of electrotactile stimulation. Of the five subjects three identified the correct pixel at a rate above chance. As previously described, a bipolar configuration could be used to increase accuracy but would require higher voltages to induce sensations of tingling.

4.4.4 Human subject experiments with electropneumotactile device

To assess human subjects' abilities to perceive mechanical and electrical stimuli at the same time, we integrated a fluidic control board (Soft Robotics toolkit) with the function generator and linear amplifier (Figure S3). The fluidic control board controlled the position and amplitude of pneumatic stimulation with a pump, four pressure sensors, and four valves. A series of mechanical relay switches controlled the position of the

electrotactile stimulation. Finally, an Arduino microcontroller and custom code were used to control both actuators.

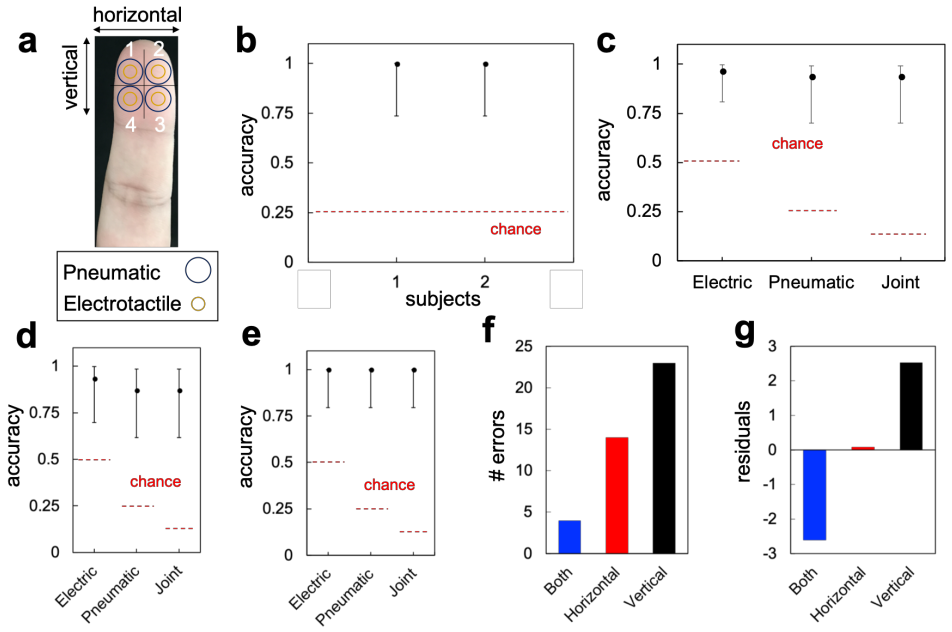

Figure 5. Psychophysical experiments using the electropneumotactile device. (a) Diagram of electrotactile and pneumatic pixel locations on the figure tip. (b) Individual subject accuracy when discriminating between four pneumatic pixels. Error bars are 95% confidence intervals (Clopper-Pearson method for exact binomial confidence intervals) (c) Overall accuracy for human subject perception of electrotactile (electric) stimulators and pneumatic actuators, and for joint performance (correct only if subject judged both stimulation types correctly). Error bars are Wald 95% confidence intervals on fixed effects of logistic mixed effect regression model. Red line depicts chance performance. (d) First subject's performance and (e) second subject's performance. Error bars are 95% confidence intervals (Clopper-Pearson method for exact binomial confidence intervals). The red dotted line depicts chance performance. (f) Counts of each type of error (g) Depiction of the residuals of the χ^2 test.

Figure 5a shows the pneumatic and electrotactile actuator positions used for human subject testing. Figure 5b shows the individual accuracy of two subjects whom were asked to identify the position of pneumatic stimulation between four pixels. Both subjects correctly identified the position of blister inflation with 100% accuracy.

While subjects showed the ability to identify both electrical (Figure 4b) and mechanical (Figure 5b) stimuli independently, it is unclear from these results alone whether subjects are able to perceive both stimuli at the same time. Figure 5c shows the combined results of two subjects who were blindfolded and asked to determine the location (pixel #1-4) of pneumatic stimulation and whether there was electrotactile stimulation (yes/no). In the case where electrotactile stimulation was on, the location of electrotactile stimulation always coincided with the pneumatic pixel that was inflated. The results show that both subjects correctly identified the combined stimuli at rates significantly higher than chance. Individual subject results are broken down in Figures 5d and 5e. Figure 5f shows the number count of error types (horizontal, vertical, or both) that subjects made. A vertical error is characterized between confusing pixel #1 for #3 or pixel #2 for #4 (and vice versa), while a horizontal error was the result of subjects confusing pixel #1 for #2 or pixel #3 for #4 (and vice versa) (Figure 5a). Qualitatively, subjects made errors in the vertical position (23 errors) more than in the horizontal position (14 errors). In addition, subjects rarely made both errors simultaneously (4 errors). This difference was statistically significant ($\chi^2(2) = 13.22, p = 0.0013$). Figure 5g depicts the residuals of the chi-squared test. Residuals larger than 2 indicate a statistically significant contribution, suggesting that subjects made more vertical errors than expected, and also fewer diagonal (horizontal and vertical) errors than expected, under the null hypothesis that all errors should be equally-likely. The ability of subjects to identify electrotactile stimulation while a pneumatic actuator was inflated supports the premise that the electro-mechanical properties of PEDOT/PU enable multi-modal haptic sensations.

4.5 Conclusion

In this work, we introduce an electropneumotactile device that delivers multimodal haptic actuation. Dual delivery of mechanical and electrical stimulation is achieved by combining a compliant stretchable conductor with a pneumatic actuator. While pneumatic actuators and electrotactiles are common forms of stimulation in haptic devices, these two stimuli have not been previously combined due to a mismatch in mechanical behavior. This demonstration is part of a larger effort within our laboratory to use the tools of organic materials chemistry in haptics research—"organic haptics." This approach has already led to new strategies for haptic feedback[29] and has enabled mechanistic studies[30,31] on touch perception.

Chapter 4, in part is currently being prepared for submission for publication of the material. Carpenter, C.W.[1], Rodriquez[1], D., Tan, S.T.M., Root, N.B., Malinao, M., Skelil, K., Ramírez, J., Polat, B., Root, S.E., Ramachandran, V.S., Lipomi, D.J. The dissertation author was the primary investigator and author of this material.

4.6 References

[1] X. Wu, H. Zhu, S. Kim, M. G. Allen, *IEEE Transducers Eurosensors* **2007**, 1409.

[2] T. S. Hansen, K. West, O. Hassager, N. B. Larsen, *Adv. Funct. Mater.* **2007**, *17*, 3069.

[3] V. Yem, H. Kajimoto, *2017 IEEE Virtual Real.* **2017**, 99.

[4] S. Hasegawa, M. Konyo, K. Kyung, T. Nojima, H. Kajimoto, *Haptic Interaction*; 2018.

[5] C. W. Soule, N. Lazarus, *Smart Mater. Struct.* **2016**, *25*, 1.

[6] H. Kwon, S. W. Lee, S. S. Lee, *Sensors Actuators A Phys.* **2009**, *154*, 238.

[7] N. Besse, S. Rosset, J. J. Zarate, H. Shea, *Adv. Mater. Technol.* **2017**, *1700102*, 1.

[8] Y. Qiu, Z. Lu, Q. Pei, *ACS Appl. Mater. Interfaces* **2018**, *10*, 24807.

[9] D. R. Merrill, M. Bikson, J. G. R. Jefferys, *J. Neurosci. Methods* **2005**, *141*, 171.

[10] K. A. Kaczmarek, J. G. Webster, P. Bach-y-Rita, W. J. Tompkins, *IEEE Trans. Biomed. Eng.* **1991**, *38*, 1.

[11] K. A. Kaczmarek, *Sci. Iran.* **2011**, *18*, 1476.

[12] M. Štrbac, M. Belić, M. Isaković, V. Kojić, G. Bijelić, I. Popović, M. Radotić, S. Došen, M. Marković, D. Farina, T. Keller, *J. Neural Eng.* **2016**, *13*, 046014.

[13] S. Dosen, M. Markovic, M. Strbac, M. Beli, G. Bijeli, T. Keller, D. Farina, S. Member, *IEEE Trans. Neural Syst. Rehabil. Eng.* **2017**, *25*, 183.

[14] M. Franceschi, L. Seminara, S. Dosen, M. Strbac, M. Valle, D. Farina, S. Member, *IEEE Trans. Haptics* **2017**, *10*, 162.

[15] K. A. Sluka, D. Walsh, *J. Pain* **2003**, *4*, 109.

[16] M. Ying, A. P. Bonifas, N. Lu, Y. Su, R. Li, H. Cheng, A. Ameen, Y. Huang, J. A. Rogers, *Nanotechnology* **2012**, *23*, 344005.

[17] S. Lim, D. Son, J. Kim, Y. B. Lee, J. Song, S. Choi, D. J. Lee, J. H. Kim, M. Lee, T. Hyeon, D. Kim, *Adv. Funct. Mater.* **2015**, *25*, 375.

[18] S. E. Root, C. W. Carpenter, L. V Kayser, D. Rodriquez, D. M. Davies, S. Wang, S. T. M. Tan, Y. S. Meng, D. J. Lipomi, *ACS Omega* **2018**, *3*, 662.

[19] L. V Kayser, D. J. Lipomi, *Adv. Mater.* **2019**, *1806133*, 1.

[20] J. Y. Oh, S. Kim, H. Baik, U. Jeong, *Adv. Mater.* **2016**, *28*, 4455.

[21] L. V Kayser, M. D. Russell, D. Rodriquez, S. N. Abuhamdieh, C. Dhong, S. Khan, A. N. Stein, J. Ram, D. J. Lipomi, *Chem. Mater.* **2018**, *30*, 4459.

[22] D. Khodagholy, T. Doublet, M. Gurfinkel, P. Quilichini, E. Ismailova, P. Leleux, T. Herve, S. Sanaur, C. Bernard, G. G. Malliaras, *Adv. Mater.* **2011**, *23*, 268.

[23] M. Sessolo, D. Khodagholy, J. Rivnay, F. Maddalena, M. Gleyzes, E. Steidl, B. Buisson, G. G. Malliaras, *Adv. Mater.* **2013**, *23*, 2135.

[24] D. Khodagholy, J. N. Gelinas, Z. Zhao, M. Yeh, M. Long, J. D. Greenlee, W. Doyle, O. Devinsky, G. Buzsáki, *Sci. Adv.* **2016**, *2*, 1.

[25] M. Ganji, E. Kaestner, J. Hermiz, N. Rogers, A. Tanaka, D. Cleary, S. H. Lee, J. Snider, M. Halgren, G. R. Cosgrove, B. S. Carter, D. Barba, I. Uguz, G. G. Malliaras, S. S. Cash, V. Gilja, E. Halgren, S. A. Dayeh, *Adv. Funct. Mater.* **2017**, *1700232*, 1.

[26] J. Kim, A. Nizami, Y. Hwangbo, B. Jang, H. Lee, C. Woo, S. Hyun, T. Kim, *Nat. Commun.* **2013**, *4*, 1.

[27] D. Rodriquez, J. Kim, S. E. Root, Z. Fei, P. Bou, M. Heeney, T. Kim, D. J. Lipomi, *Appl. Mater. Interfaces* **2017**, *9*, 8855.

[28] M. A. Alkhadra, S. E. Root, K. M. Hilby, D. Rodriquez, F. Sugiyama, D. J. Lipomi, *Chem. Mater.* **2017**, *29*, 10139.

[29] C. W. Carpenter, S. Ting, M. Tan, C. Keef, K. Skelil, M. Malinao, D. Rodriquez, M. A. Alkhadra, J. Ramírez, D. J. Lipomi, *Sensors Actuators A. Phys.* **2019**, *288*, 79.

[30] C. W. Carpenter, C. Dhong, N. B. Root, D. Rodriquez, E. E. Abdo, K. Skelil, M. A. Alkhadra, J. Ramírez, V. S. Ramachandran, D. J. Lipomi, *Mater. Horizons* **2018**, *5*, 70.

[31] C. Dhong, L. V Kayser, R. Arroyo, A. Shin, M. F. Iii, A. T. Kleinschmidt, D. J. Lipomi, *Soft Matter* **2018**, 7483.